A Contribution to the Structure of Coals from X-Ray Diffraction Studies

L. Cartz and P. B. Hirsch

Email alerting service	Receive free email alerts when new articles cite this article - sign up in the box at the top right-hand corner of the article or click **here**

[557]

A CONTRIBUTION TO THE STRUCTURE OF COALS FROM X-RAY DIFFRACTION STUDIES

By L. CARTZ and P. B. HIRSCH

Crystallographic Laboratory, Cavendish Laboratory, Cambridge

CONTENTS

Detailed X-ray diffraction studies have been carried out on a series of vitrains, anthracites, lignites, durains, fusains and certain coal extracts, of varying rank. The results are interpreted in terms of a basic structural model in which the carbon atoms are arranged in small aromatic layers linked to each other by aliphatic or alicyclic material or by five-membered rings to form large buckled sheets. Data have been obtained on the layer size distributions, the average layer diameters, the average bond length, the proportion of amorphous material and on the nature of the packing. The significance of the various structural parameters deduced from X-ray data is discussed critically. All the results are considered together in an attempt to develop as detailed a structural model as possible. The nature of the coalification process and the structural differences between various macerals are discussed and the results are compared with those deduced from other studies.

1. Introduction

Some years ago a study of the X-ray scattering from a series of vitrains of varying rank (Hirsch 1954) led to the conclusion that coals with less than 89 % carbon consist of rather small aromatic layers containing only a few condensed rings, and that while some of these are packed parallel to one another in groups of two or three, a considerable proportion of the layers occurs singly. The scattering at very low angles did not support the existence of a micellar structure, but suggested a wide distribution of anisotropic pores.

Since that time further advances have been made in the interpretation of X-ray patterns (Diamond 1956, 1957, 1958; Cartz, Diamond & Hirsch, unpublished). Accordingly the series of vitrains has been re-examined, using the new techniques of analysis, and the work has been extended to a variety of other materials, including a series of anthracites, lignites, micrinite, exinite, durains and fusains of varying rank, and some coal extracts. The object of this paper is to report on the results obtained, and to discuss critically the information about the structure of coals which can be deduced. Some preliminary results have been reported previously (Cartz, Diamond & Hirsch 1956; Hirsch 1958); the results on the carbonization of coal are reported by Diamond in an earlier paper (1959), which will be referred to as III.

2. Nature of the X-ray scattering

Figure 1 shows typical diffraction patterns for three vitrains of 78 % C, 89 % C and 94 % C, respectively, as a function of s $(=(2 \sin \theta/\lambda)$, where θ is half the scattering angle, and λ is the wavelength). The intensity curve is corrected for polarization. This X-ray pattern can be considered conveniently in several parts.

(1) The scattering at high angles consists of diffuse bands similar to the two-dimensional diffraction bands (10, 11, 20, etc.) obtained from pure amorphous carbons. Accordingly these high-angle bands are interpreted in terms of the scattering from small condensed aromatic layers.

(2) The scattering at intermediate angles consists of a band (002) corresponding to a spacing of $\sim$ 3·5Å in the case of vitrains. Again, by analogy with the scattering from carbons, this band is considered to be due to the packing of the layers parallel to one another. For some coals this band is replaced by one at higher spacings, the γ band, and this is thought to be due to the closest distance of approach of rather badly buckled molecules in these coals (Cartz *et al.* 1956).

(3) At low angles intense diffuse scattering occurs for the low-rank vitrains at angles corresponding to spacings of $\sim$ 20Å up to at least several 1000Å. This scattering is thought to be due to macropores (Hirsch 1954). For many coals there is comparatively little scattering between this region and the 002 band. For certain types of coals a weak band appears in the region of 20Å (see figure 1 *b*) and this band must be due to a change in density of the structure on this scale. The particular interpretation for vitrains has been discussed by Brown & Hirsch (1955).

The diffraction patterns of all coals and related materials are similar in that they all show these three types of scattering. However, they differ from each other with respect to the breadth and position of each band, and also with respect to the nature and intensity of the scattering at lower angles.

Because of the similarities between the diffraction patterns of coals and that due to amorphous carbon, the patterns are first interpreted in terms of a model of perfect aromatic layers of different sizes packed parallel to each other to a varying degree of order. Evidence will then be presented about the imperfections in the model, and an attempt will be made to interpret the results as far as possible in terms of a more realistic model.
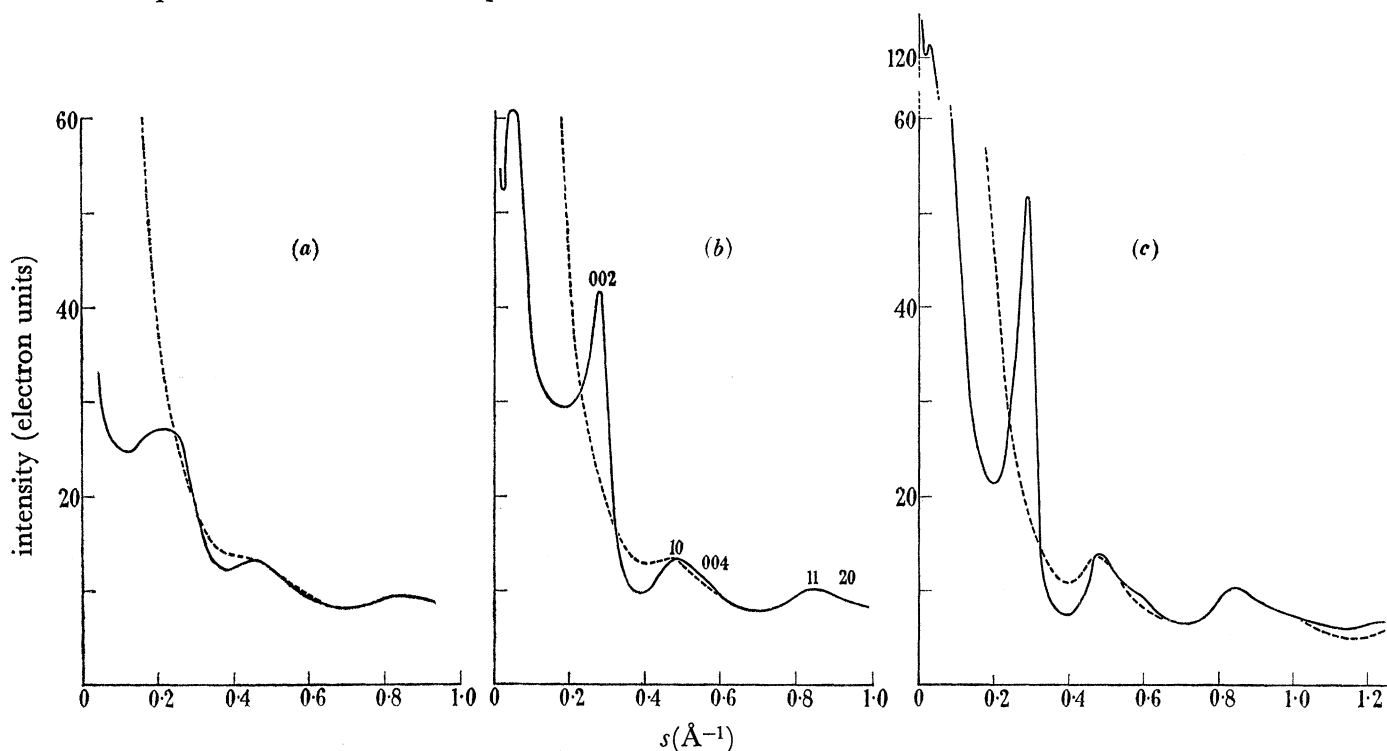

FIGURE 1. The X-ray diffraction patterns for three typical vitrains of (a) 78 % carbon, HA; (b) 89 % carbon, HE, and (c) 94 % carbon, HM. The intensity is on an absolute scale (electron units) per carbon atom, and is plotted as a function of s ($= 2 \sin \theta / \lambda$). The dashed curve in each case is the theoretical curve fitted in the region of $0 \cdot 66 \leqslant s(\text{Å}^{-1}) \leqslant 0 \cdot 96$; see §4. The continuous line is the experimentally determined curve; in the case of the coal HM of 94 % carbon, the intensity increases continuously with decreasing angle in the low-angle range not shown.

3. EXPERIMENTAL PROCEDURE

The X-ray diffraction patterns were obtained photographically with crystal-reflected $\text{Cu}K\alpha$ radiation. At high and intermediate angles an evacuated 9 cm diameter powder camera was used, covering a range of s from $\sim 0 \cdot 20$ to $\sim 1 \cdot 20 \text{Å}^{-1}$. At low and intermediate angles an evacuated symmetrical transmission type focusing camera (see Peiser, Rooksby & Wilson 1954) with a plastically bent lithium fluoride monochromator was used, and the diffraction pattern recorded from $s \sim 0 \cdot 02$ to $\sim 0 \cdot 40 \text{Å}^{-1}$. The experimental procedures and conditions, specimen preparation and other details were similar to those described by Diamond (III).

4. DETAILED INTERPRETATION OF THE SCATTERING AT HIGH ANGLES

4·1. Method of interpretation

As described in §2, the scattering is considered to be due partly to perfect aromatic layers, and partly to independently scattering ('amorphous') atoms. The analysis due to

Diamond (1957, 1958, III) is used, in which a linear combination of theoretical intensity curves from small layers of different sizes (figure 2) and from 'amorphous' atoms is fitted to the experimental curves over a range extending from $0 \cdot 66$ to $0 \cdot 96 \text{Å}^{-1}$ by the method of least squares. By means of a matrix transformation, the distribution of layer diameters and the proportion of 'amorphous' material are derived (and usually displayed in histogram form) as well as a value for the average bond length. Generally, two photographs were obtained from each specimen; comparison of the histograms obtained from these two photographs shows that the shape of the distribution is significant (Diamond 1958). The
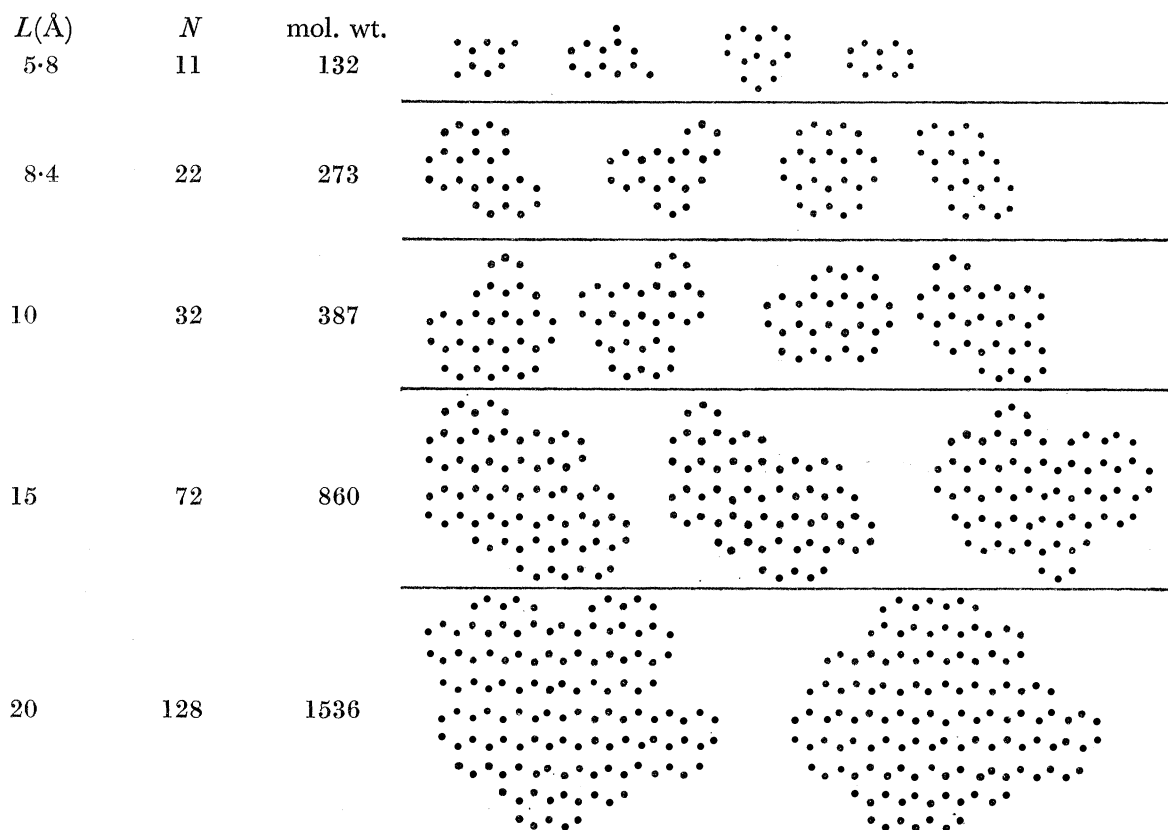
$L(\text{Å})$	N	mol. wt.
5·8	11	132
8·4	22	273
10	32	387
15	72	860
20	128	1536

FIGURE 2. The sizes of the layers, L (Å), used in the analysis of the high-angle diffraction pattern; a further layer size of $L = 30 \text{Å}$ containing 288 carbon atoms is not shown. The relation between L, the layer size, and N, the number of carbon atoms per layer, is given in §4·5 of the text.

average histogram has been recorded in each case. The average layer diameter, $\bar{L}$, is usually accurate to $\sim 0 \cdot 2 \text{Å}$ and the relative values of bond lengths are accurate to $\sim 0 \cdot 002 \text{Å}$ (see Diamond 1958, III). The absolute values of bond lengths are somewhat too low owing to certain systematic errors. Thus, no absorption correction was applied to the experimental intensity curves; the linear absorption coefficient, μ, was measured directly on coal slabs by transmission using a Geiger-counter spectrometer and was found to be $\sim 7 \cdot 5 \text{ cm}^{-1}$ for most of the coals used. The appropriate value of μr for specimens of radius $r = 0 \cdot 4$ mm used in the powder cameras is therefore $0 \cdot 32$. Since the absorption factor from a cylindrical specimen varies with angle of scattering (Bradley 1935), this can lead to a displacement of the diffraction peak. Calculations show that neglect of this absorption correction causes the bond length of a low-rank coal (80 % C) to be too low

by $\sim 0.003\,\text{Å}$, and of a high-rank coal (90% C) by $\sim 0.0015\,\text{Å}$. While this error must be present there is another possible source of error due to shrinkage of the film during the exposure in the vacuum camera (we are indebted to Dr G. J. Pitt for pointing out this source of error). Tests on film shrinkage have shown that this error can cause the bond lengths to be too low at most by $0.0015\,\text{Å}$.* The most accurately determined term of the histograms is that due to 'amorphous' material, but it may be influenced considerably by the presence of non-carbon atoms (see III). Figure 3 shows a typical histogram obtained in this way from a vitrain of 94% C; the various terms correspond to those of figure 2, to
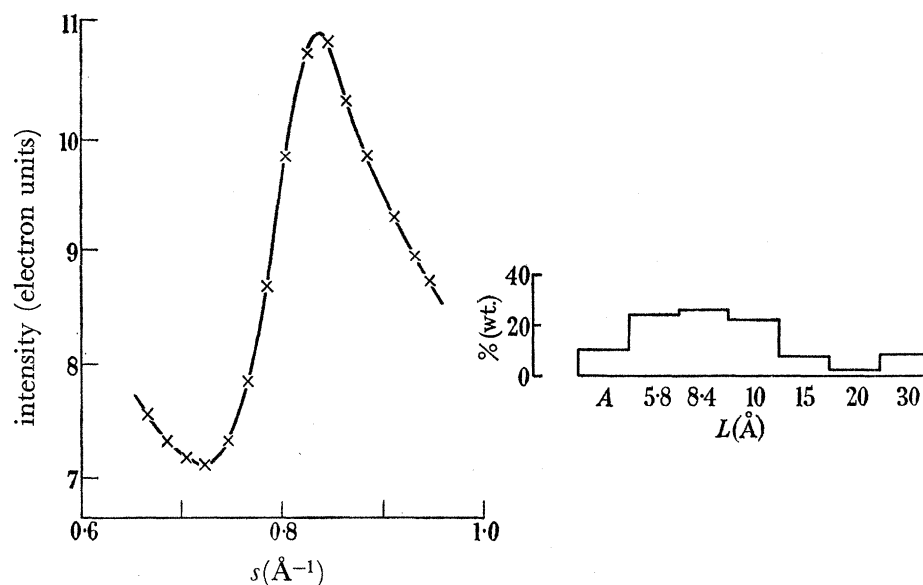

FIGURE 3. A typical histogram of layer sizes is shown for the anthracite HM of 94% carbon. The first term A of the histogram gives the proportion of independently scattering carbon atoms, and the other terms give the proportion of carbon in layers of the sizes indicated (see figure 2). The average layer diameter, $\bar{L}$, defined in the text in §4·1 is $10.7\,\text{Å}$ and the average bond length, l, $1.407\,\text{Å}$. The diagram also shows the experimental curve (continuous line) used in the analysis and the theoretical curve (crosses) corresponding to the histogram.

an additional size group $L = 30\,\text{Å}$, and to the amorphous material (A). The average layer diameter, $\bar{L}$ (defined by the relation $\bar{L} = \Sigma \lambda L / \Sigma \lambda$, where λ is the proportion of carbon in layers of size L), and bond length l are also given. Figure 3 also shows a comparison of the theoretical curve corresponding to this histogram with the experimental curve (see also figure 1c). The agreement over the range of fitting ($0.66 < s < 0.96\,\text{Å}^{-1}$) is good.

4·2. The discrepancies

Outside the range of s in which the fitting is carried out the experimental and theoretical curves diverge (figure 1). The discrepancy at higher values of s is probably partly due to inaccuracies in the values of Compton scattering used in the analysis; while fluorescent radiation from small amounts of Fe impurities could also produce such deviations, similar discrepancies have been found in carbonized coals (see Diamond III) and in a specially prepared pure amorphous carbon. (We are indebted to Dr J. K. Brown for the preparation

---

* We are indebted to M. Augoyat of St Gobain (Paris) for carrying out these tests.

of this sample; for details see appendix I.) In the present work the values of Compton scattering tabulated by Compton & Allison (1935), not corrected for the Breit–Dirac relativistic recoil factor, have been used throughout. In fact Diamond (III) has shown that if the recent calculations of Compton scattering due to Keating & Vineyard (1956) are used, and if the appropriate absorption correction ($\mu r = 0\cdot3$) is applied to the experimental intensity curves, this discrepancy disappears, provided the Breit–Dirac factor is not included in the values of Compton scattering (see III for further discussion).
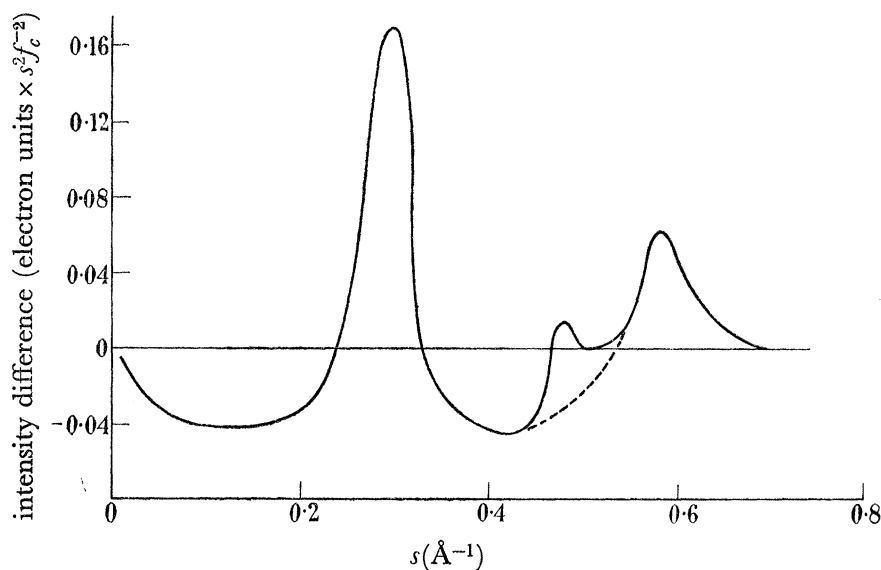

FIGURE 4. The difference between the theoretical and experimental scattering curves for an anthracite HM of 94 % carbon. This is obtained from figure 1 (c) by multiplying the difference in electron units by $s^2 f_c^{-2}$. Note the peak in the region of the 10 band. For the analysis of the 00l scattering, the effect of this '10 discrepancy' is removed by extrapolation as shown (dashed line).

A more serious discrepancy occurs at lower angles in the region of the 10 band. Most o the difference between the calculated and experimental curves is due to the 00l intensity variation due to the packing of the layers. If the assumption of perfect condensed aromatic ring systems were correct, the difference curve would be solely due to the 00l intensity distribution. Figure 4 shows such a difference curve obtained from figure 1 c; the difference curve has been multiplied by $s^2 f_c^{-2}$ (f_c = atomic scattering factor of carbon) for convenience. While most of the curve in the region of the 10 band is due to the onset of 004 band, a small contribution still remains from the 10 band; this is the small peak in figure 4 at $s \sim 0\cdot5\,\text{Å}^{-1}$. This means that the 10 band is more intense or sharper than it should be *and indicates that the layers are really larger than assumed, but imperfect.* The magnitude of the discrepancy amounts to $\sim 0\cdot5$ electron unit compared with ~ 13 electron units for the total height of the 10 band for a low-rank vitrain, and $\sim 1\cdot6$ for the high-rank anthracite HM (see table 1). Thus, even the larger layers are imperfect, and as Diamond (III) has shown, the imperfections are also important after carbonization to 1000 °C. While the existence of imperfections in the layers has been established, it is, however, not possible at present to make any quantitative predictions about the nature of the imperfections from the magnitude of the discrepancy.

There is a further discrepancy at even lower angles. Thus, for a low-rank vitrain the breadths of the bands at high angles indicate that the coherently diffracting layers can only be about 7 Å in diameter. Some of these layers are packed parallel to each other in small groups; however, if there were real gaps in the structure around the periphery of the layers, there would be strong low-angle scattering in the range of angles corresponding to a spacing of about 14 Å or greater. In actual fact the intensity in this range of angles ($s \sim 0.07\,\text{Å}^{-1}$) is found to be less than about 20 % of that expected from independently scattering layers. This can be seen from the intensity curves plotted on an absolute scale (electron units) in figure 1. On this scale at $s \sim 0.07\,\text{Å}^{-1}$ the intensity should be approximately $\frac{1}{2}Nf_c^2$, where N is the number of atoms per layer and f_c is the atomic scattering factor

TABLE 1. DISCREPANCIES IN THE REGION OF THE 10 BAND

coal	% C	magnitude of discrepancy (electron units)
vitrains		
HA	78·3	0·6
HB	80·1	0·5
HC	84·4	0·5
HD	87·3	small
HE	89·0	0·9
HF	89·3	0·9
HH	91·4	0·6
HM	94·1	1·6
fusains		
HZ	91·4	1·2
DA	93·1	0·8
micrinite concentrate		
HY	86·5	0·4
pitch		
DO	92·7	1·2
co-precipitate of three quinones		
—	—	1·0

The height of the 10 band for all these materials is about 13 electron units.

for carbon. For coal HA (figure 1a) this should be about 234, whereas the actual intensity is only about 27 electron units. The corresponding figures for coal HE (figure 1b) are 324 and 57 electron units, respectively. For the anthracite the value of $\frac{1}{2}Nf_c^2$ should be reached at $s \sim 0.05\,\text{Å}^{-1}$ since the layers are rather larger; here the corresponding figures are 651 and 120 electron units, respectively. Thus in all cases the scattering is only a small fraction of that expected from independently scattering layers of diameter derived from the high-angle bands. In this respect the diffraction patterns from coals differ from those from amorphous carbons, where the low-angle scattering is larger in this range of angles; this is evident, for example, from the low-angle scattering curve from an amorphous carbon described by Franklin (1950, figure 2; see also Franklin 1951).

It follows immediately that in the coals the small layers must be situated adjacent to each other, so that little change of density occurs outside their coherent range. This is confirmed by the similarity of the diffraction patterns of coals and related materials to that of a co-precipitate of three quinones (see §§4·5, 7·7; also figure 24) where there is no doubt that the molecules are packed in this manner. This result is entirely in accord with the

above conclusion that the layers are in reality larger than deduced from the high-angle diffraction pattern, but imperfect. The model which suggests itself is one of imperfect and buckled sheets consisting of small condensed aromatic ring systems which are intimately linked to each other in such a way that the hexagons are rotated relative to each other to destroy the coherence of scattering. The question arises whether these buckles or changes in orientation occur at definite chemical groupings as, for example, at alicyclic bridges or five-membered rings (as in fluorene), or whether the sheets are wholly aromatic but bent and twisted merely elastically perhaps as a result of steric hindrance (Robertson 1953). We believe that both types of imperfection are likely to occur. In the next section the influence of certain particular types of imperfections which might occur will be discussed.

4·3. *The meaning of the layer diameter $\bar{L}$ and of the 'amorphous' term A*

The preceding discussion suggests that the layers are really *imperfect* and form part of larger units. However, the quantitative interpretation is carried out in terms of *perfect* layers. If the imperfections are due to particular chemical groupings, the question arises as to the type of chemical grouping which leads to a break in the coherence of scattering and which effectively terminates the layer contributing to the region of the 11, 20 bands. Calculations of the effect of particular molecular configurations discussed in detail in III have led to the following conclusions.

(1) Edge atoms in the form of CH_2 or CH_3 groups contribute completely to the size of the layer, $\bar{L}$, and partly, to the extent of about 50% of their weight, to the 'amorphous' material. (The contribution to A depends on $\bar{L}$; the above figure is appropriate to $\bar{L} \sim 8\cdot5\,\text{Å}$; for further details see III.)

(2) Independently scattering oxygen atoms contribute heavily (according to their atomic weight) to the term corresponding to the 'amorphous' material; it is clear from table 3 in III that, if most of the oxygen atoms are scattering independently, much of the amorphous material may be due to oxygen atoms in the low-rank coals. There is little doubt from other evidence, e.g. infra-red spectroscopy, that some of the oxygens occur as edge groups attached to aromatic systems, so that the contribution of oxygens to the 'amorphous' material will be rather smaller, but at present no quantitative estimates are possible. Independently scattering oxygen atoms may also cause an apparent lowering of the term in the histogram due to the smallest size group. This might lead to inaccuracies in $\bar{L}$, particularly for the oxygen-rich lignites.

(3) Five-membered rings in small layers may contribute almost completely to the value of $\bar{L}$; in larger units five-membered rings terminate the layer (see Diamond (III) for the actual molecules considered).

(4) Buckles due to hydroaromatic groups terminate the layers.

(5) Elongated layers give rise to a wide distribution in the histograms.

(6) Layers containing holes give rise to bimodal distributions in the histograms.

It follows that when the layer diameters, $\bar{L}$, deduced from the experiments are interpreted in terms of definite models containing condensed aromatic rings, care must be taken to allow for the presence of edge atoms and of possible other configurations, such as five-membered rings. It is clear that the calculations on particular molecular shapes and configurations have not been exhaustive, and much remains to be done here to define more

clearly the type of configuration which might be included in this determination of $\bar{L}$. The 'amorphous' material may be interpreted reasonably in terms of 'edge' atoms, and perhaps short aliphatic chains, but it should be emphasized that no exact correlation is possible with the fraction of non-aromatic or aliphatic material obtained from other measurements (Brown 1955; Van Krevelen & Chermin 1954 a, b; Brown & Hirsch 1955; Van Krevelen & Schuyer 1957). If such correlations are attempted they can only be used to show trends. This point will be discussed again in §7·1.

If the imperfections are due to general elastic strains, such as bending or twisting of the molecules, all that may be said about $\bar{L}$ is that it represents a lower limit of the actual size of the *imperfect* sheet and an upper limit of the size of the *perfect* region of the layer. To give an idea of the order of magnitude of the possible strain effect we quote the result of a calculation by Diamond (1956) of the diffraction pattern from a layer of diameter 20 Å with a Gaussian strain distribution, so that the uncertainty of position of a given atom relative to any other atom is proportional to the distance r between these atoms; and r.m.s. error of the position of an atom r relative to an origin atom was chosen to be $0\cdot069r$, and the effective layer diameter $\bar{L}$ in the 11, 20 region was found to be 9·78 Å, i.e. about half the true diameter of the layer. The 10 band is of course considerably sharper, and this gives rise to a discrepancy similar to that found in the coals. The actual value of the discrepancy was found to be 3 electron units. Although this discrepancy is somewhat larger than that found for the coals (see table 1), and although the strains need not be of the same type as in this case, the example serves to show that such strains can give rise both to a considerably smaller $\bar{L}$ and to a discrepancy in the 10 region. Thus, a discrepancy of ~ 1 electron unit as found for some of the coals would be consistent with the view that the diameter of the larger imperfect layers exceeds the value of $\bar{L}$ by about 2 to 3 Å.

It is quite clear from the above discussion that the layer of diameter $\bar{L}$ cannot necessarily be identified with the coal molecule as determined by other measurements such as molecular weight determinations (for references see Dryden 1958) or by statistical structural analysis (Van Krevelen & Schuyer 1957; Dryden 1958). Because of this difficulty the word 'molecule' will be avoided in this paper and the term 'layer' is used to describe the unit of diameter $\bar{L}$ which diffracts effectively coherently in the 11, 20 region. This 'layer' is considered to be part of a larger structure probably in the form of a buckled imperfect sheet which may correspond to Dryden's 'cluster unit' (Dryden 1958).

4·4. *Bond-length measurements*

With Diamond's analysis it is possible to determine the mean bond lengths between the atoms in the layers. These measurements can be used to deduce additional information about the structure of the layers. The average C—C bond lengths in some small aromatic molecules and certain other bond lengths of interest are shown in table 2. This table shows clearly that the average bond lengths of small aromatic molecules increase rapidly with the number of rings in the molecule. Since edge groups around isolated layers are known to diffract coherently with the rest of the layers, the different bond lengths of these groups will cause a change of the average bond length of the layer. Diamond (III) has in fact correlated certain bond-length changes on carbonization with structural changes. So far, however, no extensive calculations exist which might give reliable quantitative estimates

of the bond length change due to a given edge group. Furthermore, since the layers are cross-linked to form larger structures which may be in the form of buckled imperfect sheets, the average bond length may be effectively decreased owing to the deviation of the

TABLE 2. SOME KNOWN BOND LENGTHS IN ORGANIC STRUCTURES

type of bond	molecule	no. of rings	(Å)
C—C	benzene	1	1·39
C—C	naphthalene	2	1·40
C—C	anthracene	3	1·404
C—C	pyrene	4	1·41
C—C	graphite	∞	1·42
C—C	(aliphatic)		1·54
C—OH	(hydrogen bonded)		1·36
C=O			1·215
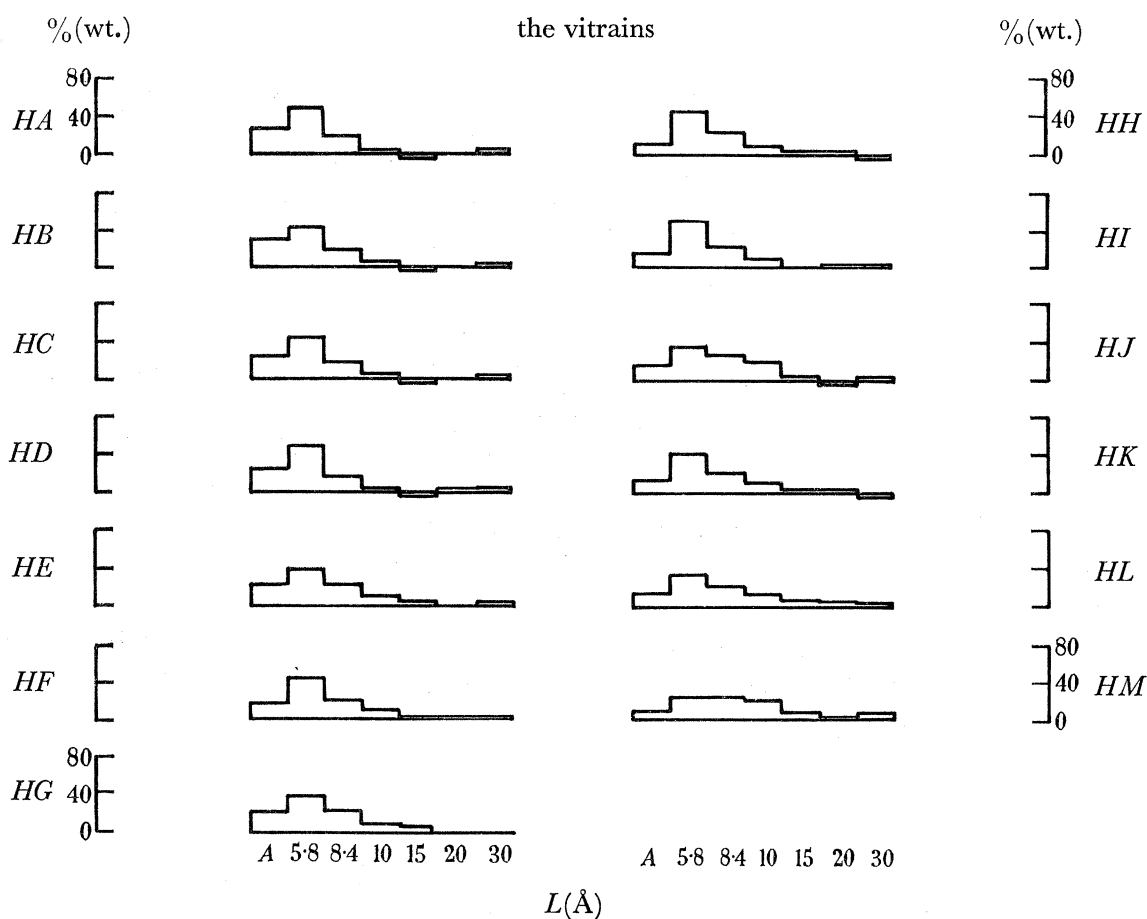
FIGURE 5. The layer-size histograms for the vitrains.

hexagons out of a plane. To a first approximation the effective bond length will probably be the projection of the bond lensgth in the bent layer on a mean plane. In spite of these uncertainties, the bond length measurements can be used to exclude certain molecular configurations and changes of bond lengths with varying rank can be discussed at least qualitatively in terms of changes in chemical structure.

4·5. *Results*

The histograms obtained from a variety of coals and related materials (vitrains, durains, fusains, lignites, ethylene diamine extracts, a pitch and an 'artificial coal') are presented in figures 5 to 9, 13, 14. The analyses and numerical data are given in appendixes I and II, respectively. The variations with carbon content of the mean layer diameter $\bar{L}$, the average number of atoms per layer $\bar{N}$, the average bond length l, and the proportion of amorphous

FIGURE 6. The layer-size histograms for the lignites and a lignin.

material A, are shown in figures 10 to 12. The layer diameters L are defined in terms of the number of atoms N per layer by the relation: $L = 2 \cdot 5 \sqrt{(\frac{1}{2}N)}$ (see Diamond 1957). This definition is clearly arbitrary, as the linear dimension of a layer must be related to N in a manner depending on its shape. According to the above definition L is the side of a 60° rhombus whose sides are parallel to the sides of the unit cell of a plane graphitic sheet; this unit cell is obtained by joining the mid-points of four adjacent benzene rings as in pyrene, and the side of this unit cell has been taken as $2 \cdot 5 \text{Å}$ (an approximation to the actual unit cell side of graphite of $2 \cdot 46 \text{Å}$). The average number of atoms $\bar{N}$ is obtained from $\bar{L}$ by using the above formula.
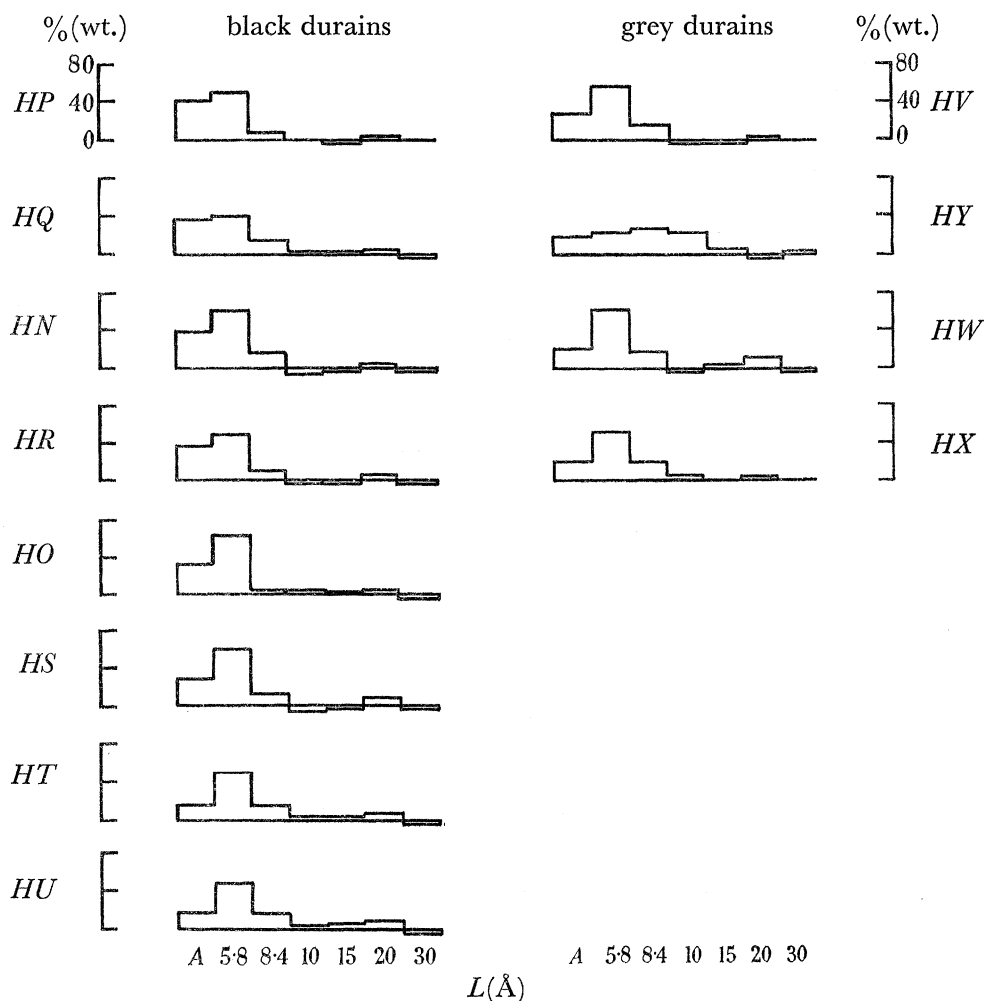
FIGURE 7. The layer-size histograms for the durains.
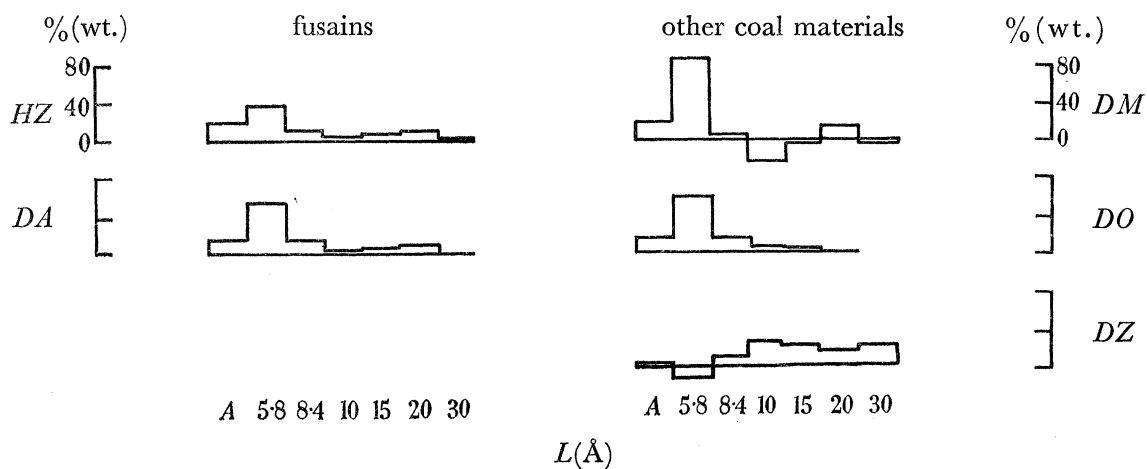
FIGURE 8. The layer-size histograms for the fusains and some other coal substances.
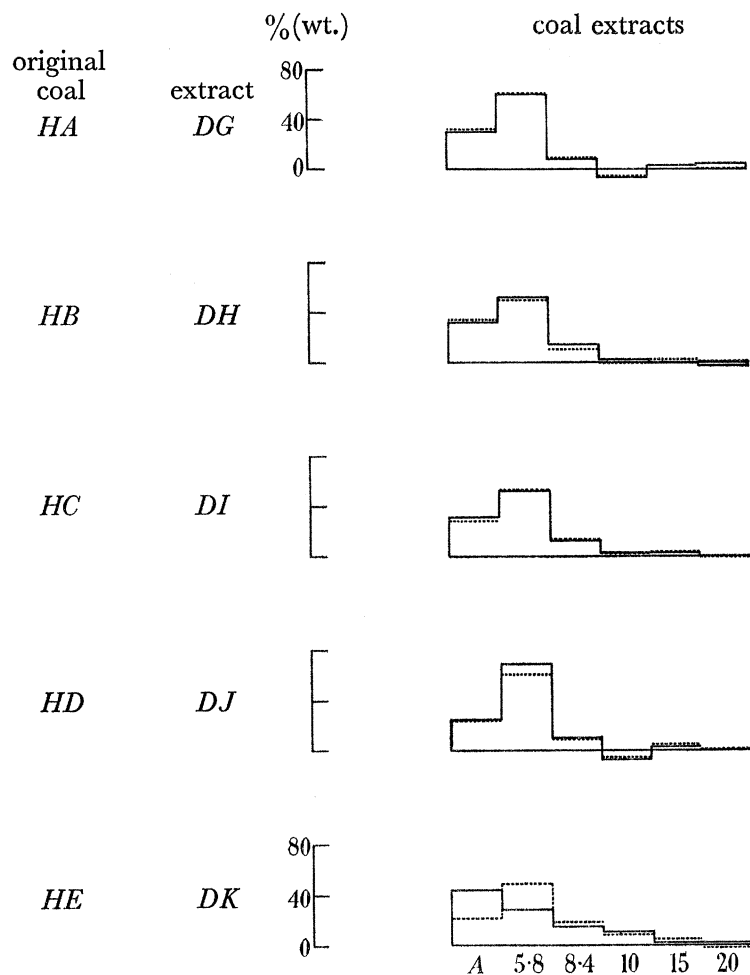
FIGURE 9. Comparison of the coal extracts with the corresponding original coals. The histograms of layer sizes are given of both the original coal (dashed) and the extract (solid lines). An earlier matrix prepared by Diamond was used, in which the largest layer size was 20 Å.
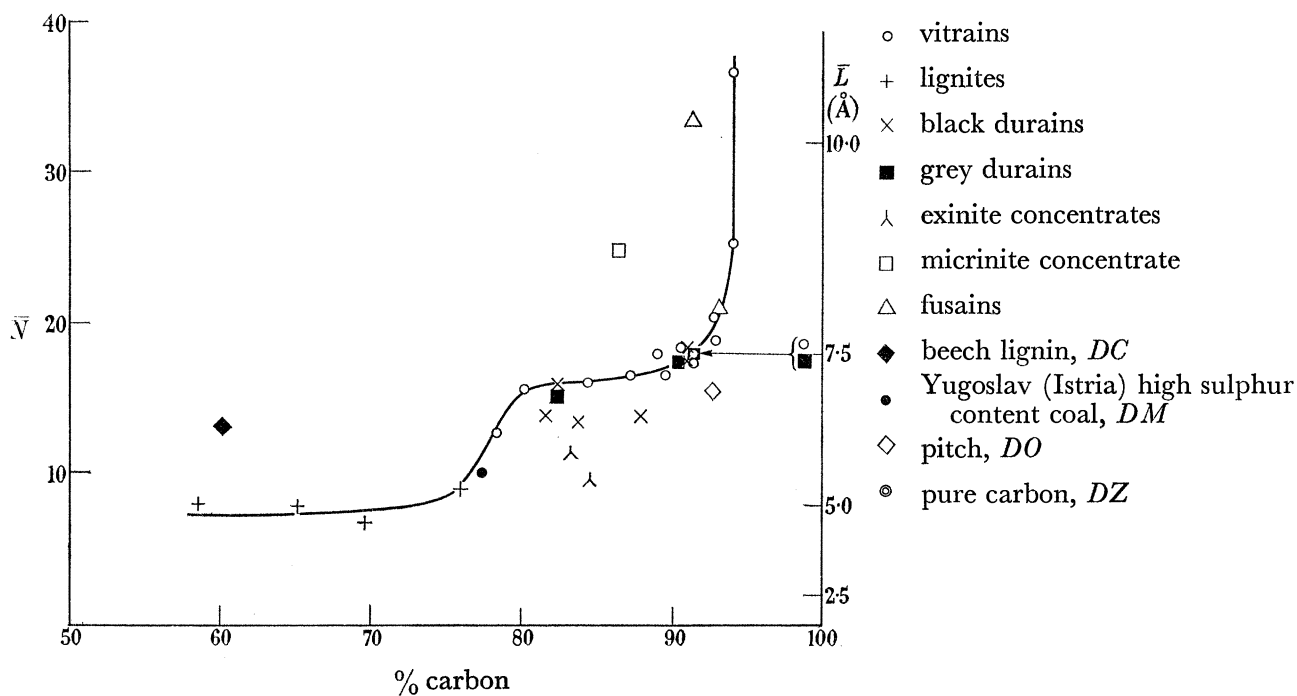
FIGURE 10. The variation of the average layer diameter, $\bar{L}(\text{Å})$, and the average number of atoms per layer $\bar{N}$, with carbon content. The curve refers to the lignites and vitrains only. The same symbols are used in figures 10, 11 and 12.
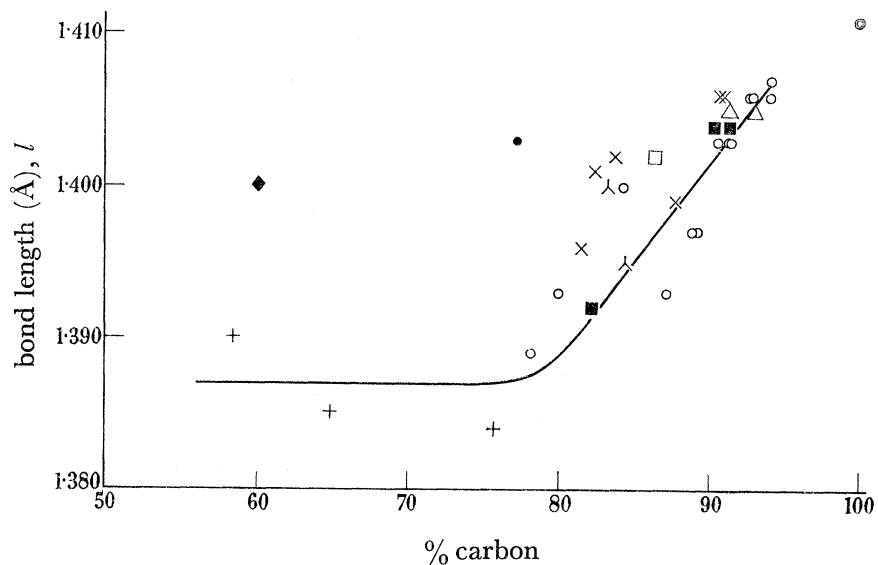
FIGURE 11. The variation of the bond length, l, with carbon content. The curve refers to the lignites and vitrains only. The bond-length measurements are somewhat less accurate for the lignites than for all other coals.
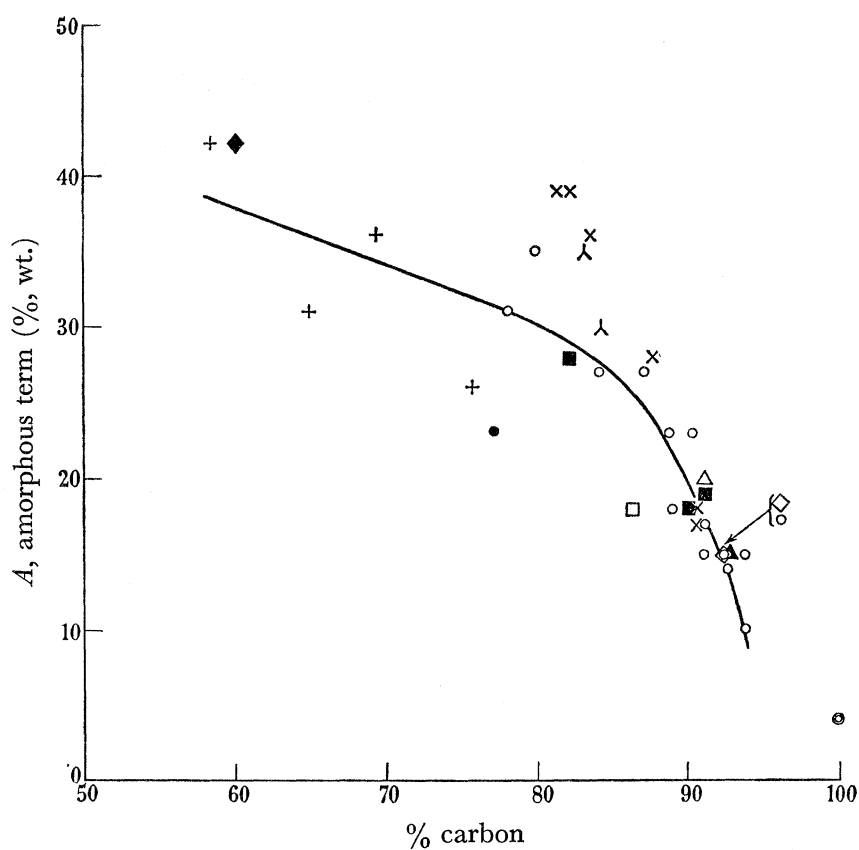
FIGURE 12. The variation of the amorphous term, A, with carbon content. The curve refers to the lignites and vitrains only.

The vitrain series includes those previously studied by Hirsch (1954), and was provided by Dr G. W. Fenton (Coal Survey Laboratory, Sheffield). Some of the coals contained a comparatively large amount of mineral matter; it was found possible to remove this by treatment with a mixture of dilute hydrochloric and hydrofluoric acids (carried out at the
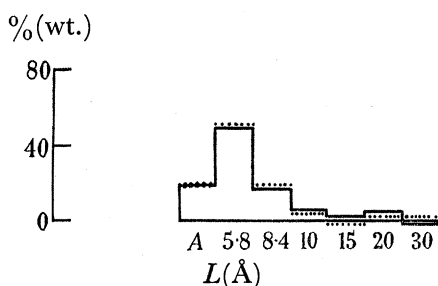
FIGURE 13. The layer-size histogram of a grey durain, HX, before (solid line histogram) and after (dotted histogram) treatment with acids to remove mineral matter. The bond length was also found to be essentially unchanged. $l = 1 \cdot 404$ Å (before), $1 \cdot 405$ Å (after treatment); $\bar{L} = 7 \cdot 5$ Å (before), $7 \cdot 3$ Å (after treatment).
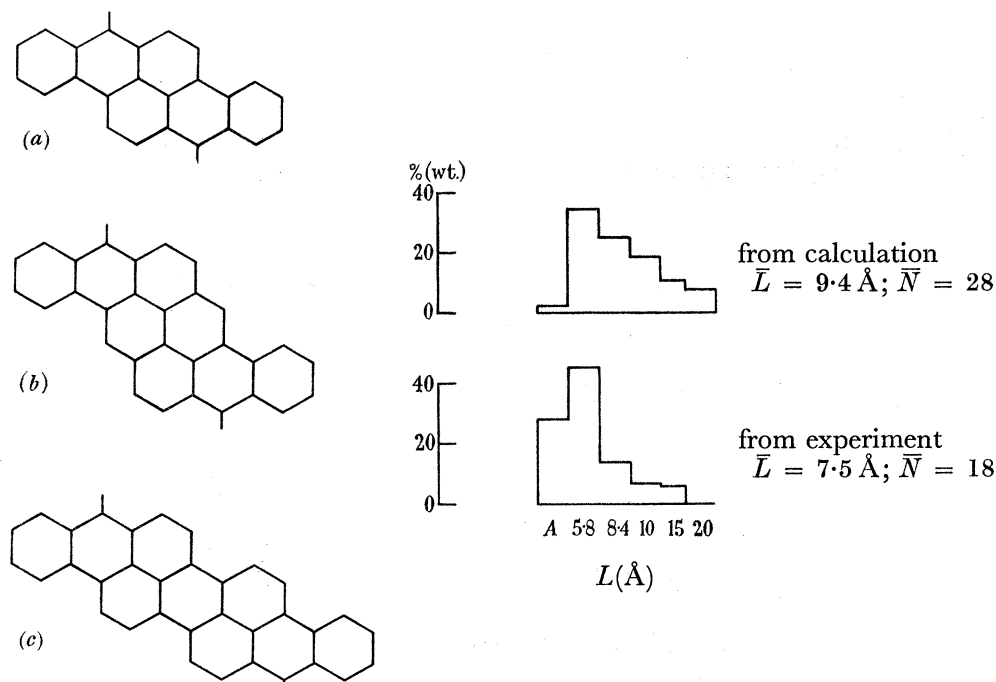
FIGURE 14. The 'artificial coal' prepared from the three quinones: (a) $1':2':6':7'$: dibenzpyrene-7:14 quinone; (b) pyranthrone; (c) isodibenzanthrone. Histograms of layer sizes are shown for the analysis of the experimental curve, and of the calculated scattering curve assuming a random array of pyranthrone molecules (pyranthrone contains 30 carbon atoms, 2 of oxygen and 14 of hydrogen and the mean of the three molecules contains 29 carbon atoms, 2 of oxygen and 14 of hydrogen). The earlier matrix prepared by Diamond was used in which the largest layer size was 20 Å.

Coal Survey Laboratory, Sheffield). This treatment did not seem to affect the coal structure, since the results were always similar to those of untreated vitrains of similar rank; in the case of a grey durain, HX, it was possible to determine the layer-size histogram before and after treatment, and, as shown in figure 13, these are approximately the same.

The durains examined are all mixtures of exinite, micrinite, and vitrinite (see appendix I); however, it was possible to obtain one specimen of almost pure micrinite, and two of almost pure exinite (see appendix I for source of these materials). The ethylene diamine extracts of the vitrain coals (Dryden 1951 a, b, c, 1952) were provided by the British Coal Utilization Research Association. Only part of the vitrain will dissolve in this solvent, the

TABLE 3. DATA ON LOW-ANGLE DIFFRACTION BANDS

material	spacing (Å)	intensity relative to that of 002 band (divided by f_c^2)
vitrains with carbon content above $\sim 86\%$ C; particularly pronounced in range 89 to 92 % C (figure 1); similar bands for durains containing micrinite or vitrinite of comparable rank; rather weak bands for fusains (for vitrains see Hirsch 1954)	~ 20	comparable
ethylene diamine extract DK of HE (probably not representative of coal; Cartz et al. 1956; figure 4b)	~ 34	weak band superimposed on heavy low-angle scattering
ethylene diamine extracts DG, DH of HA, HB (Cartz et al. 1956; figure 4a).	~ 12	weak
ethylene diamine extract DI of HC	~ 16	weak
lignites DD, DE (figure 25)	~ 12	weak
lignin DC	~ 10	weak
pitch DO (figure 23d)	~ 10	weak
co-precipitate of three quinones (figure 24)	$\sim 8\cdot3$, ~ 11, ~ 15	weak

TABLE 4. ANALYTICAL DATA OF SAMPLE OF PITCH (DO)

(Supplied by Professor Van Krevelen.)

		%
elementary analysis	C	92·7
	H	4·4
	O	0·4
	N	1·2
	S	0·9
density (helium)		1·30 g/cm³
density (mercury)		1·29 g/cm³
refractive index		1·93
aromaticity ($f_{ar.}$)		0·89
rings per C-atom ($(R-1)/C$)		0·27
size of aromatic cluster ($C_{ar.}$)		27

solubility decreasing with increase of carbon content. For most of the extracts considerable fractions of the original coal could be extracted. Thus extract DI represents about 35 % of the original coal (HC). In the case of vitrain HE, however (89 % C) only about 1 % could be extracted (DK), and this may not therefore be representative of the original material. The histograms shown in figure 9 have been obtained using an earlier matrix prepared by Diamond in which the largest layer size was 20 Å.

The lignites were obtained from various sources indicated in appendix I.

The sample of pitch was provided by Van Krevelen and the structural parameters determined for this material by Van Krevelen and his colleagues, using statistical structural analysis, are given in table 4.

The 'artificial coal' was prepared as follows. Akamatsu & Nagamatsu (1947) reported that when three brightly coloured quinones (1':2':6':7':dibenzpyrene-7:14 quinone, pyranthrone and *iso*dibenzanthrone; for structure see figure 14) are co-precipitated from sulphuric-acid solution, a black amorphous powder is obtained. Such material was prepared according to the above prescription from equimolecular proportions of quinones provided by I.C.I. (reference numbers E25608, E25602 and E25605, respectively) and was carefully washed and dried after preparation. The quinones were stated to have possibly up to 10 or 20% impurities in the form of quinones of lower molecular weight. (We are indebted to Dr J. K. Brown for help in preparing this coprecipitate.) The X-ray diffraction pattern from this material was found to be similar to that of coals in that it consists mainly of the two-dimensional bands at high angles and of a 002 band at intermediate angles. (A simple mixture of the quinones gives normal crystalline reflexions.) At lower angles some bands appear at spacings corresponding to the packing of the molecules adjacent to each other in the plane of the molecules (see §7·7). The two-dimensional bands at high angles were analysed in the usual way by the matrix method; the histogram is shown in figure 14.

All these results will be discussed together with those obtained from the lower-angle diffraction patterns in §7.

5. The scattering at intermediate angles

5·1. *Method of interpretation*

At intermediate angles, in the region of $s \sim 0.2$ to $0.4\,\text{Å}^{-1}$, the diffraction pattern arises from the packing of the layers. In the case of the vitrains the main feature is the 002 band, interpreted by analogy with pure carbons as being due to stacking of parallel layers. More
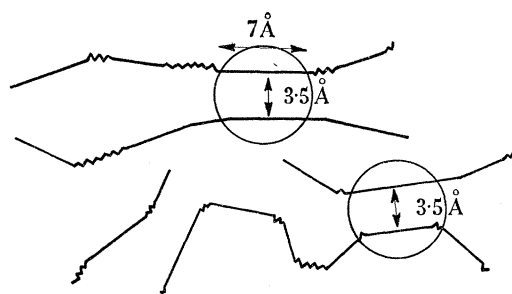
FIGURE 15. A schematic representation of packing of locally flat regions of the buckled layers; see §5·1. The circles indicate the size of the nucleus of the unit responsible for the '20 Å' band; see §7·1.

precisely, in terms of the model of buckled sheets proposed in §4·3, the 002 band is thought to be due to the parallel packing of locally flat regions of these sheets, as shown schematically in figure 15. The scattering curves are analyzed by Fourier transformation according to the method of Cartz, Diamond & Hirsch (to be published). Briefly, the theoretical intensity curve representing the scattering from the distribution of single randomly oriented layers appropriate to the histogram of the particular coal is subtracted from the experimental scattering curves in the region of the 002 and 004 bands, the difference

giving essentially the distribution of intensity in the 002 and 004 bands, apart from a residual contribution of the 10 band already referred to (see §4·3, table 1 and figure 4). This latter contribution is smoothed out and the resulting curve is transformed by Fourier analysis.

The transform of the difference curve for the anthracite *HM* is shown in figure 16. This transform has been adjusted so that the minimum between each peak is zero. As a result of this adjustment and of a 'smoothing out' of diffraction ripples the intensity and shape of the first peak are not accurately determined, and this leads subsequently to errors in the proportion of single layers and of those arranged in pairs (full details of this method will be given by Cartz, Diamond & Hirsch elsewhere).
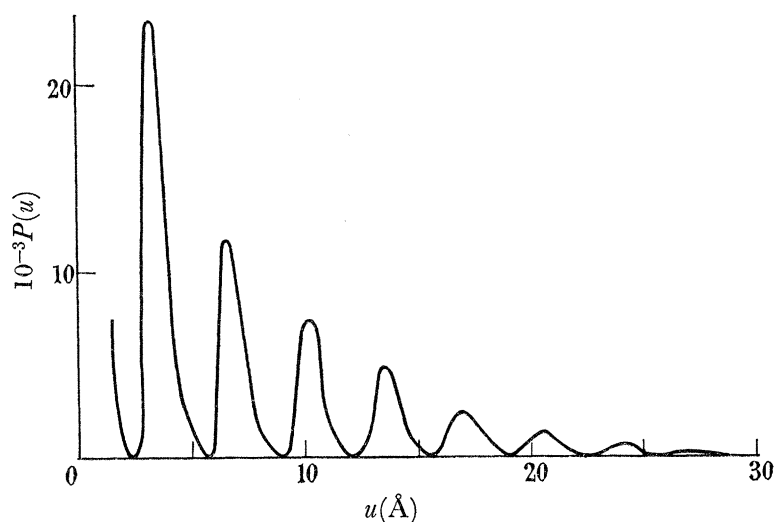
FIGURE 16. The transform of the difference curve of the anthracite coal *HM* of 94 % carbon; see §5·1 and figure 4. $P(u)$ gives the probability of finding another layer at a distance $u(\text{Å})$ from any layer in the coal.

The transform (for example, figure 16) gives the probability $P(u)$ of finding another layer at a distance u from any layer in the coal. The breadth of each peak is due to a variation in the separation between layers; the width at half height of each peak can be used as an estimate of the magnitude of this variation. The position of the maximum gives the most probable separation; a mean value of the most probable separation is found by averaging the ratio of distance from the origin to the peak to the number of that peak counted from the origin. From the areas under the peaks the relative numbers of layers in stacks of 2, 3, etc., are obtained by a double difference method (Hirsch 1954). Since the intensity curves, and therefore the Fourier transforms, are on an absolute scale, the origin peak in the transform is known, and using this value the proportion of single layers is derived. In this analysis it is assumed that the amorphous material (the term A of the histograms of figures 5 to 9) does not take part in the parallel packing of the layers, so that the origin peak is proportional to $(1-A)$.

This assumption may not be justified; in fact the proportion of carbon in single layers deduced in this way may be considered as a lower limit. An upper limit would correspond to the case in which all the amorphous material takes part in the parallel packing. An approximate estimate of this upper limit may be obtained by adding A to the value of the

lower limit. The true proportion of carbon in single layers probably lies between these two extreme values.

It is thus possible to determine from the transforms the relative proportions of layers in stacks of varying sizes, the most probable distance from any layer to another layer, and the variation in the separation of the layers.

5·2. Results

In figures 17 and 18 the histograms of the packing of the layers are given for the series of vitrains and for two fusains, a micrinite concentrate and a pitch.

The numerical data for these histograms are given in appendix III. An average number of layers per stack, $\bar{n}$, is also given; $\bar{n}$ is defined by the relation $\bar{n} = \Sigma p / \Sigma(p/n)$, where p is the fraction by weight of layers in stacks of n layers. The average interlayer spacing, $\bar{d}$, and the
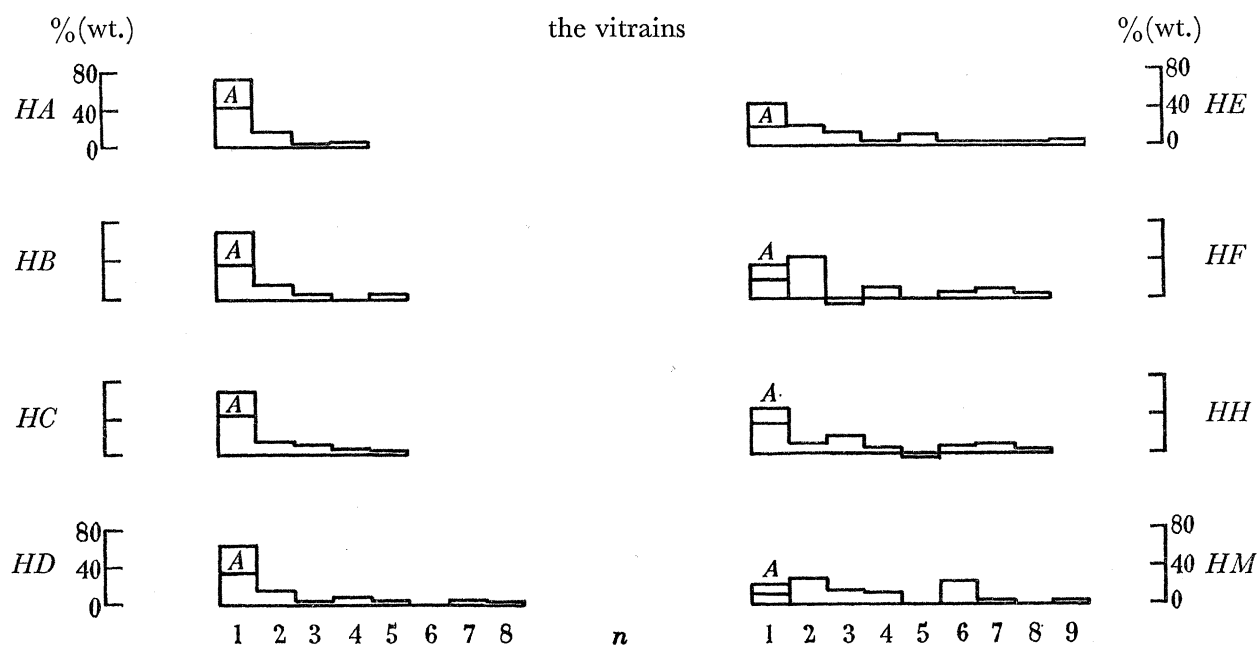
FIGURE 17. Histograms of the packing of the layers for the series of vitrains. Each histogram gives the percentage by weight of carbon present in stacks of n layers. The first term gives upper and lower limits of the proportion of carbon in the form of single layers, the two limits differing by the amount of amorphous material, A; see §5·1 for discussion.
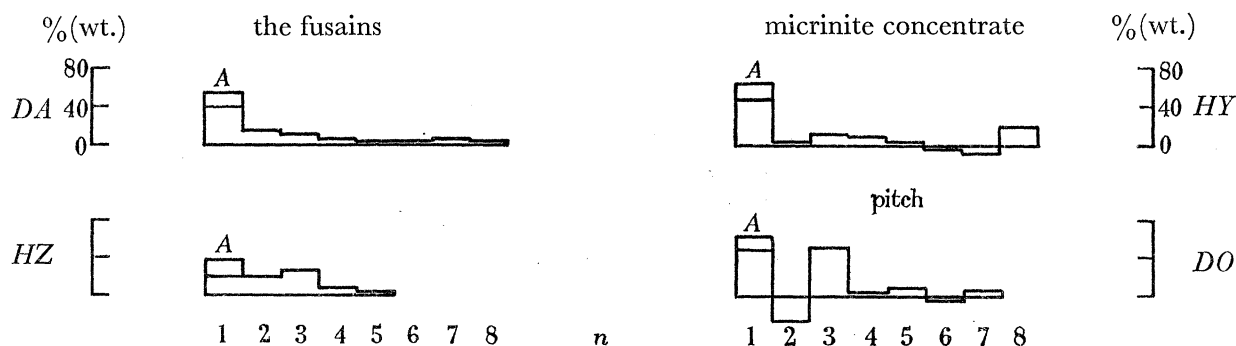
FIGURE 18. Histograms of the packing of the layers for two fusains, a micrinite concentrate and a pitch; see legend of figure 17 for explanation.
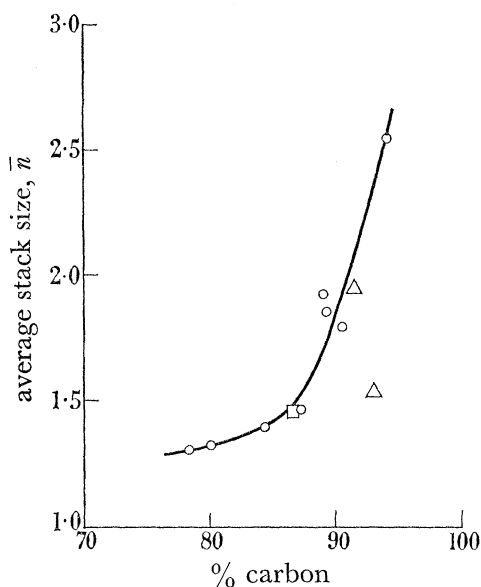
FIGURE 19
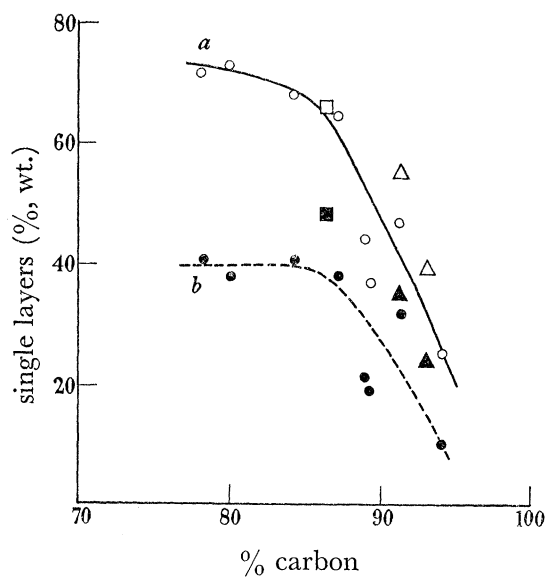
FIGURE 20

FIGURE 19. The dependence on carbon content of the average number of layers in a stack, $\bar{n}$. The curve represents the variation for the vitrains only. The circles designate the vitrains, the triangles the fusains and the square the micrinite concentrate.

FIGURE 20. The dependence on carbon content of the proportion of carbon in single layers: (a) Upper limit, open symbols and solid curve; (b) lower limit, filled-in symbols and dotted curve. The curves give the variation for the vitrains. The circles represent the vitrains, the triangles the fusains and the square the micrinite concentrate.
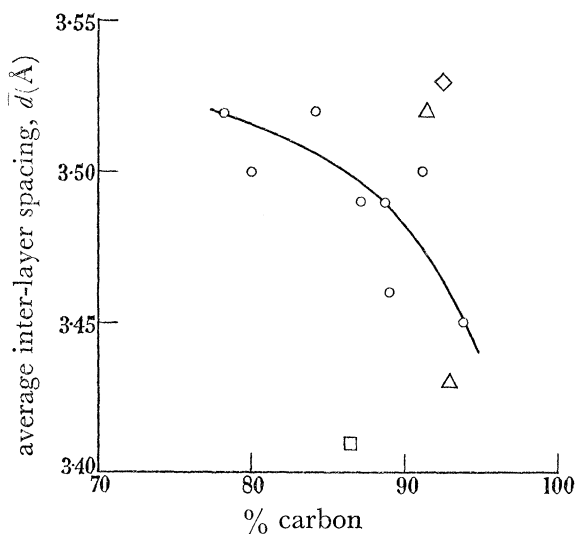
FIGURE 21
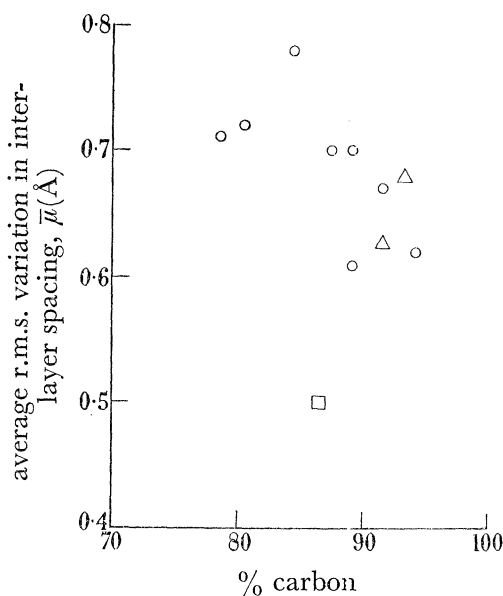
FIGURE 22

FIGURE 21. The dependence on carbon content of the average interlayer spacing, $\bar{d}$. The circles represent the vitrains, the triangles the fusains, the diamond the pitch and the square the micrinite concentrate. The curve gives the variation for the vitrains.

FIGURE 22. The dependence on carbon content of the average r.m.s. variation in interlayer spacing $\bar{\mu}$. The circles represent the vitrains, the triangles the fusains and the square the micrinite concentrate.

average root-mean-square variation, $\bar{\mu}$, of the interlayer spacing (derived from the breadth of the peaks in the transform by fitting a Gaussian-type curve to each peak) are also tabulated.

The dependence on carbon content of the average number of layers in a stack, $\bar{n}$ is shown in figure 19. A similar curve for the proportion of carbon in single layers is shown in figure 20, where a second curve is given in which the amorphous term, A, obtained from the analysis of the two-dimensional diffraction bands at higher angles (appendix II) has been added. The variation with carbon content of the average interlayer spacing $\bar{d}$ is given in figure 21 and that of the average root-mean-square variation in interlayer spacing $\bar{\mu}$ in figure 22.

In the case of the black durains (appendix I) this analysis has not been attempted, since for most of these the main feature is the γ band occurring at a spacing of 4 to 5 Å (Blayden, Gibson & Riley 1944; Nelson 1954; Cartz *et al.* 1956) which overlaps the 002 band. The γ band from an exinite concentrate (HN) is compared with the 002 from a vitrain of similar rank in figure 23*a*. In this case the 002 band of HN is very weak indeed compared to the γ band. However, most of the other black durains show a sharp 002 band superimposed on the γ band even though the proportion of micrinite is only quite small. Thus, the parent material of the exinite concentrate HN is the durain HR which contains only 13·3 % carbinite; yet the intensity curve of this material published previously (Cartz *et al.* 1956; figure 2) shows a significant 002 peak. Comparison of the intensity curves and analyses from HN and HR shows that the suppression of this peak is accompanied apparently by quite a small reduction (a few parts per cent) in the micrinite content. The peak intensity of the 002 band due to micrinite is therefore considerably greater than that of the γ band from an equivalent amount of exinite.

The grey durains (appendix I) show a sharp 002 band but no γ band. The Fourier transform method has been applied to the micrinite concentrate (HY), the low- and intermediate-angle diffraction pattern of which is compared with that of a vitrain of similar carbon content in figure 23*b*. The 002 band of the micrinite is seen to be rather sharper than and displaced to higher angles relative to that of the vitrain. The histogram is shown in figure 18.

The fusains also show a 002 band; an example (HZ) is shown in figure 23*c* where the low- and intermediate-angle diffraction pattern is compared with that of a vitrain of similar carbon content (HH). The 002 of the fusain appears to be rather broader than that of corresponding vitrain, but the real difference is in the shape of the bands rather than in their average breadths. The histograms obtained from the Fourier transforms from the fusains are shown in figure 18. Comparison of the histograms from HZ and HH shows in fact that the distribution in the latter is much wider than in the former, as expected from the shapes of the diffraction bands. The mean number of layers per stack is, however, similar for both.

The sample of pitch (DO) also shows an 002 band, and its diffraction pattern is compared with that of a vitrain of comparable carbon content in figure 23*d*. The histogram is shown in figure 18.

All these materials show 002 bands (other 002 bands have been published by Hirsch (1954); Nelson (1954); Cartz *et al.* (1956)) which are considerably broader than that from the

co-precipitate of three quinones, whose low-angle diffraction pattern is shown in figure 24. The spacing of the peak of this 002 band is $\sim 3 \cdot 35 \text{Å}$, equal to that in graphite. Although the Fourier transform method has not been applied in this case, the shape of the band, in particular the presence of a sharp peak and of wide tails, suggests that the distribution in the histogram would be very broad.
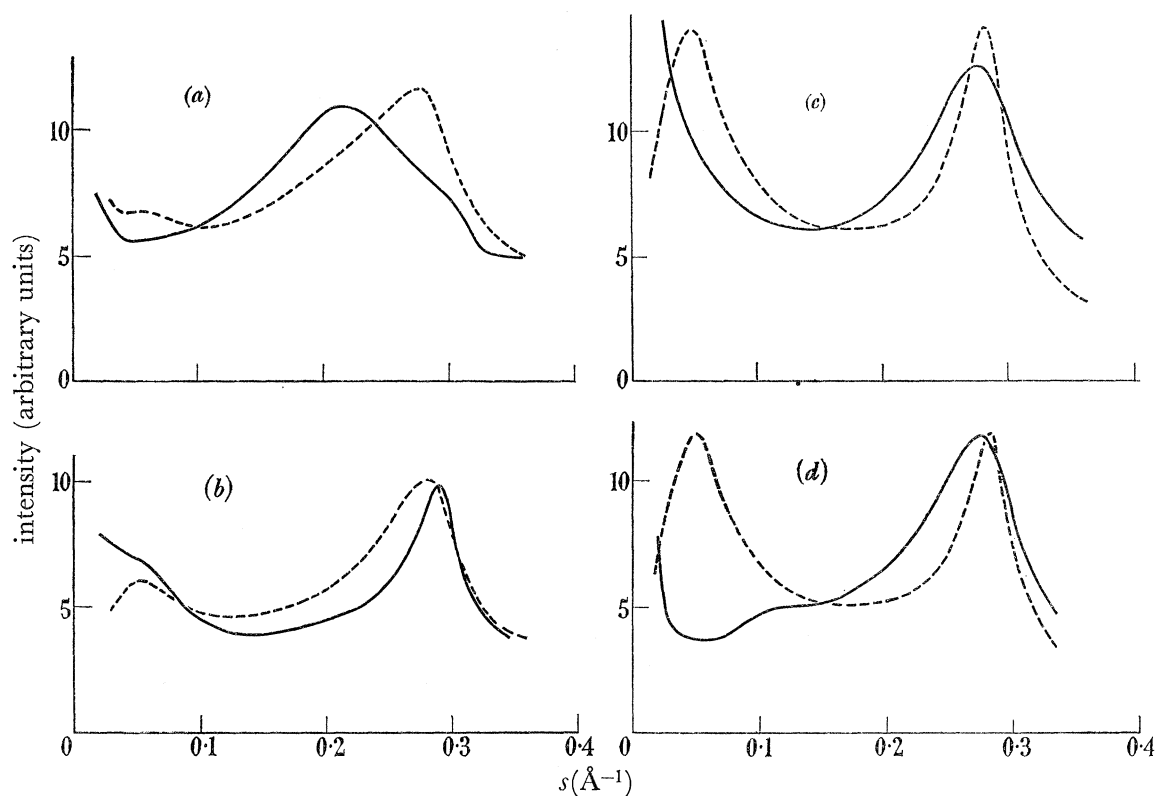
FIGURE 23. The low-angle X-ray scattering from an exinite, a micrinite, a fusinite and a pitch compared with that of vitrains of similar carbon content. (a) Exinite concentrate, HN (solid curve) and vitrain HC (dashed curve); (b) micrinite concentrate, HY (solid curve) and vitrain HD (dashed curve); (c) fusain HZ (solid curve) and vitrain HH (dashed curve); (d) pitch DO (solid curve) and vitrain HH (dashed curve).

The lignites show a very diffuse band in the region of $s \sim 0 \cdot 23$ to $0 \cdot 27 \text{Å}^{-1}$, corresponding to spacings $4 \cdot 35$ to $3 \cdot 7 \text{Å}$ (see, e.g. figure 25). With increasing rank the peak shifts towards higher angles, i.e. smaller spacings. The higher rank lignites also show the beginning of a 002 band (see figure 25, DF). No Fourier analysis was attempted on these diffraction patterns, as the interpretation of the bands in terms of parallel packed layers may be rather doubtful.

6. THE SCATTERING AT LOW ANGLES

Two types of scattering are observed at low angles: (1) Diffuse low-angle scattering in the region corresponding to 20Å or greater, which increases steeply with decreasing angle. (2) A band occurring usually at an angle corresponding to a spacing to 10 to 20Å.

The diffuse low-angle scattering may be considered to be due either to very large units or clusters occurring randomly, or to a distribution of pores in the solid. In the case of the vitrains the variation of the diffuse scattering with rank was found previously (Hirsch 1954)

to be similar to that of porosity with rank. It was suggested therefore that the diffuse low-angle scattering is due to macropores. We believe this to be true also for most of the other substances studied.

The other materials examined, fusains, durains, lignites, extracts, pitch, co-precipitate of quinones show diffuse low-angle scattering to a varying degree; this will be described and discussed together with other data in §7.
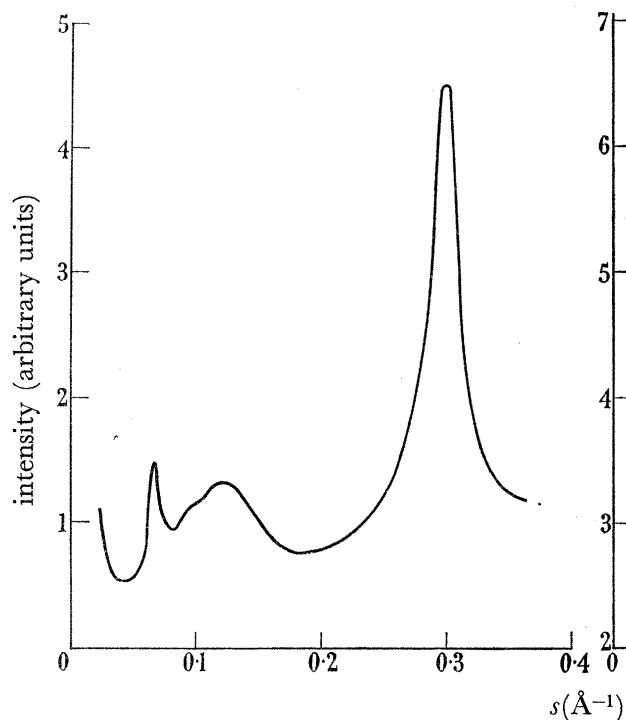
FIGURE 24. The low-angle X-ray scattering pattern from the co-precipitate of three quinones; see figure 14.
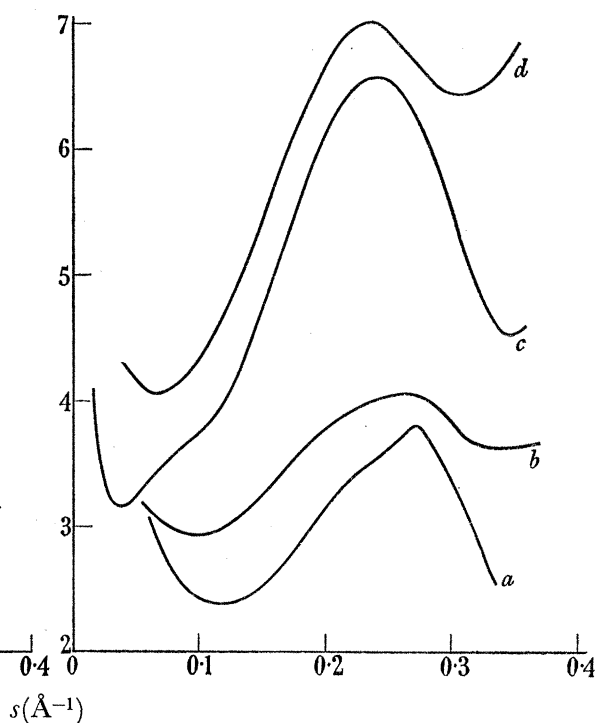
FIGURE 25. Low-angle X-ray scattering patterns of lignites. (*a*) Lignite *DB* of 58·5 % C; (*b*) lignite of 66·0 % C; (*c*) lignite *DE* of 69·5 % C; (*d*) lignite *DF* of 75·9 % C.

The bands occurring in the range of spacing 10 to 20Å are listed in table 3 for various materials. Of these the most striking is the '20Å' band for the vitrains (and durains) in the range of 90 % C. There are two possible explanations of these bands. First, the spacing of the band may be due to some repeat distance in the structure, for example, between particular groups in the molecule or between neighbouring molecules. The latter is clearly the case for the co-precipitate of three quinones (see §§4·5, 7·7; also figures 14, 24) where the bands at low angles occur at a spacing about equal to the average diameter of the molecules, and where they can be interpreted by comparison with similar reflexions from the mixture of crystals.

Secondly, the band may be due to the internal structure (a variation in density) of the unit, while the unit itself is randomly distributed in the sample. The band at 20Å in the vitrains has been interpreted in this way (Brown & Hirsch 1955). It is often not possible to determine unambiguously which of the two possibilities is the correct one. The bands will be discussed in detail in §7.

7. General discussion

In this section all the results will be discussed together to deduce as much as possible about the structure of coals and related materials and about the coalification process. The following structural parameters will be used:

1. The nature of the layer size distribution.
2. The average layer diameter or the average number of atoms per layer.
3. The fraction of amorphous material.
4. The average bond length.
5. The magnitude of the discrepancy in the region of the 10 band.
6. The nature of the packing of the layers.
7. The average number of layers in a stack of layers.
8. The average interlayer separation.
9. The variation in interlayer spacing.
10. The nature of the scattering at low angles (e.g. '20Å' band, diffuse scattering).

In order to arrive at as detailed a structural model as possible use will also be made of other data, e.g. of the elementary composition and of any information on the types of substituted edge groups available (for example, from infra-red spectroscopy).

7·1. Vitrains

It is difficult to derive a unique structural model because of the presence of imperfections (see §4·3). Assuming the plausible model of an imperfect sheet the strain may be in the form of buckles and changes of orientation about an axis normal to the layers due to chemical groups or due to elastic strains. We shall suppose that the former is rather more important and that the layer is effectively terminated at imperfections such as aliphatic or alicyclic buckles or five-membered rings (see §4·4). The reason for making this assumption derives from the existence of the band at ~ 20Å for a range of vitrains with carbon content around 90 %, from which it can be deduced (see below) that there is a unit in these vitrains of diameter ~ 8Å; this value is only slightly greater than that of $\bar{L}$ ($\sim 7\cdot5$Å for this rank) deduced from the histograms. Nevertheless, even an error of 1Å owing to strain (which is quite compatible with the magnitude of the discrepancy in the 10 region; cf. table 1) affects the model appreciably, particularly as regards the number of condensed aromatic rings in the layer. In the discussion below the histograms will first be interpreted in terms of perfect aromatic layers. There is no doubt that $\bar{L}$ represents an upper limit to the size of the perfect aromatic region. The model is then modified to allow for imperfecions.

7·1·1. Number of atoms per layer

The histograms of the vitrains are shown in figure 5. It is clear from these that for all coals, with the exception of the highest-rank anthracite, the most important term is that due to the smallest size group ($L = 5\cdot8$Å, corresponding to 11 atoms). Up to and including coal HD (87·3 % C) the histograms are fairly narrow; apart from terms A and $L = 5\cdot8$Å, the only other term of importance is that due to $L = 8\cdot4$Å. It is clear therefore that for this range of vitrains most of the layers must be small, containing only few condensed aromatic rings. The histograms are broadened a little around 89·0 % C, but most of the layers must still be very small. The histograms begin to broaden rapidly with increasing

rank after about 92% C in the anthracite region, but even for coal HL ($94 \cdot 1 \%$ C) there must still be a considerable proportion of small layers. This trend in the histograms is reflected in the variation of the average layer diameter, $\bar{L}$ (figure 10) and of the average number of atoms per layer, $\bar{N}$ (figure 10). Since it has been shown that edge atoms such as substituted aliphatic carbon atoms contribute to $\bar{L}$ or $\bar{N}$ (see §4·3), the degree of substitution must be taken into account before an estimate can be made of the average number of condensed aromatic rings per layer. The average number of atoms of the layers (assumed to be perfect) is seen to increase from ~ 13 at 78% C to ~ 16 at 84% C, ~ 18 at 90% C and ~ 37 at 94% C. Upper and lower limits of the number of rings per layer can be estimated by assuming that the layers are either completely unsubstituted or completely substituted. In this way the average number of rings is seen to lie between 1 and 3 for the low-rank vitrains and between 2 and 5 at 90% C. It is hardly likely that either of these assumptions is correct; the infra-red spectroscopy experiments (Brown 1955) suggest that the aromatic ring systems are partially substituted so that the average number of rings varies probably from 2 at 78% to 3 to 4 at 90% C. Above this carbon content the histogram is so broad that an average layer diameter or number of atoms has little significance.

It should be emphasized again that these estimates are made assuming the layers to be perfect. If they are really larger by about 1Å but imperfect, the upper limit of the number of rings, for example, at 90% C would be increased to 6.

The question has been raised (Ruland & Tschamler 1958) whether the coals really contain distributions of layer sizes as indicated directly by the histograms or whether they contain only a particular type of molecule, which, when interpreted in terms of the present model and method of analysis, gives rise to this particular histogram (for examples see III). This point cannot be decided from the results alone. It should be noted, however, that at least up to and including coal HD ($87 \cdot 3 \%$ C) the histograms are narrow and similar, and they might therefore be due to a particular type of molecule. The nature of the histogram changes somewhat between this rank and about $91 \cdot 5 \%$ C, and this change can be interpreted either in terms of a change in structure of the constituent molecule or in a broadening of the distribution of sizes. With further increase in rank in the anthracite region the histograms became so broad that there is little doubt that there must now be a wide distribution of layer diameters present. However, even in this case the apparent distribution may be exaggerated by the presence of elongated molecules (see §4·3, also III).

7·1·2. *The amorphous material*

The amorphous material is seen to decrease with increasing rank, from about 34% at 78% C to about 12% at 94% C (figures 5, 12). This decrease becomes rather more rapid after about 85% C, but this is a rather gradual change. The amorphous term is considered to be due to the substituted groups of the aromatic condensed ring systems, and may therefore be identified with the aliphatic side chains, phenolic oxygen and other substituted atoms known to be present from other lines of evidence (e.g. infra-red spectroscopy: Brown 1955). However, as those atoms which are directly linked to the layers do not contribute completely to the amorphous term, and as their contribution depends on the size of the layer (see III) it is not possible to correlate directly the amorphous material with atoms other than aromatic carbon. The presence of oxygen makes such a correlation

even more uncertain. Thus it is clear from III that if the oxygen in the low-rank coals scatters independently as amorphous material, most of the amorphous term would be due to this oxygen. Since it is known from infra-red data that there is a considerable proportion of aliphatic carbon in low-rank coals, and since this would make some contribution to the amorphous term it follows that some of the oxygen must be scattering coherently with the layers; this is in agreement with the fact that much of the oxygen is in the form of phenolic OH.

While no direct correlation is possible between the amorphous term and atoms other than aromatic carbon, the variations with rank of these quantities might be compared. The most reasonable comparison is between the fraction of aromatic carbon as determined by infra-red spectroscopy or statistical methods and the proportion of carbon in layers (i.e. $1-A$). The latter will include some oxygen and some aliphatic carbon, but the major part may be expected to be aromatic carbon. Figure 26 compares the proportion of carbon in layers with the fraction of aromatic carbon determined by infra-red spectroscopy (Brown & Hirsch 1955), from an analysis of the volatile matter of vitrinites, (Van Krevelen 1953) and from a graphical densitometric analysis (Van Krevelen & Chermin 1954b). It should be emphasized here that only the similarity of the variation with rank can be considered really significant. The agreement in magnitude between the values determined from X-ray diffraction, infra-red spectroscopy and the volatile matter is probably fortuitous.

7·1·3. *The bond lengths*

With regard to the bond-length measurements (figure 11) the gradual increase of bond length with rank is in general agreement with the gradual increase of the average layer diameter with rank. Since aliphatic and other side groups also scatter coherently with the layers, these groups will affect the average bond lengths of the layers (see §4·4). Infra-red data suggest that up to about 90% C the major change is the loss of phenolic OH accompanied by a decrease in the degree of substitution. The change in bond length due to removal of OH groups is in the same direction as that observed, but judging from table 2 this effect is probably small. It is more likely therefore that the observed increase is due to a reduction in the degree of imperfection of the layers, possibly as a result of the removal of cross-links due to hydrogen-bonded OH groups. It should also be noted that removal of an OH group will cause a reduction in $\bar{N}$, whereas the observed value of $\bar{N}$ increases slightly (see figure 10). This also suggests that in this range of carbon contents the layers are flattened slightly so as to diffract more coherently and therefore appear larger. Reference to table 1 shows that there is a tendency for the discrepancy to decrease up to about 87% C as expected. However, about this carbon content appreciable amounts of aliphatic carbon are being lost (for curve, see Brown & Hirsch 1955). Loss of an aliphatic group around the free edge of a layer would cause a decrease in the bond length (see table 2), instead of the observed increase (see figure 11). It is likely therefore that the aliphatic or alicyclic groups are removed within the layers thus causing a considerable flattening of the layers over a larger area, an increase in bond length and an increase in $\bar{L}$. It is interesting to note that the histograms are definitely broader at 89% C in agreement with this idea. If large buckles due to CH_2 groups are removed, neighbouring layers previously scattering independently may now become partially coherent; this may,

however, involve an overall increase in the degree of strain; it appears in fact from table 1 that the discrepancy increases considerably with increasing rank above this range of carbon content, becoming larger the larger the layers (a similar result was found by Diamond (III) for carbonized coals). Above 90 % the aliphatic groups are lost at a rapid rate, the histograms broaden considerably, the layer diameter increases rapidly and the discrepancy becomes very large for the highest rank anthracite (HM) (table 1). The anthracites are therefore considered to be condensed aromatic units formed by condensation within and between buckled sheets as a result of loss of aliphatic groups. A rigidly cross-linked and heavily strained (probably elastically) structure is formed and as a result large pores are created.

With regard to the absolute values of bond lengths (quoted in appendix II and recorded on figure 11) these should be corrected for the systematic errors due to absorption and shrinkage during exposure mentioned in §4·4. The correction for absorption results in an increase of the bond length of $\sim 0\cdot003$ and $\sim 0\cdot0015$ Å for the low- and high-rank coals, respectively; that for shrinkage in an increase not exceeding $\sim 0\cdot0015$ Å. However, even so the absolute values of l appear to be rather lower than expected, at least from flat perfect layers. It is true that the values of $l = 1\cdot39$ to $1\cdot40$ Å in the region 80 to 90 % C are consistent with the occurrence of single or pairs of condensed rings (see table 2) but appreciable substitution by aliphatic groups would cause these values to be larger. In any case, however, the average bond length of the high-rank anthracite would be expected to be not much smaller than that of graphite ($1\cdot417$ Å); in fact for this material l is found to be about $1\cdot4065$ (or about $1\cdot4075$ when corrected for absorption). The bond length of the pure carbon (DZ), which has much larger layer diameter than any of the coals ($\overline{L} = 18\cdot5$ Å, see figure 8) is found to be $1\cdot411$ Å; this is still below the value for graphite but considerably larger than that for any of the coals. The discrepancy of $\sim 0\cdot006$ Å for the pure carbon and an even larger one for the anthracite may be due either to an unknown systematic error which is larger the broader the diffraction band, or to the possibility that the layers are buckled and strained. Thus, the low absolute values of bond length are quite consistent with the above interpretation of the data in terms of imperfect layers.

It appears then that the results discussed so far can be explained in terms of a model (for vitrains up to ~ 90 % C) of small layers containing only a few condensed benzene rings cross-linked to form larger imperfect sheets. This model is quite consistent with the elementary analysis. Since the layers are so small it is found that the valencies can only be satisfied if the layers are extensively linked to each other either by CH_2 or alicyclic bridges or by direct C—C linkages. Extensive cross-linking is even more necessary if the models are made to fit in with the values of aliphatic and aromatic hydrogen deduced from infra-red spectroscopy (Brown 1955). Extensive cross-linking by direct C—C linkages is necessary in the case of the anthracites.

7·1·4. *The packing of the layers*

With regard to the packing of the layers, the histograms of figure 17 show that the low-rank coals contain a high proportion of single layers. As pointed out in §5·1, this fraction of single layers has not been determined very accurately; nevertheless, the trend of the values with rank may be considered to be significant. Thus below about 89 % C about 40 % of the carbon occurs as single layers, the remainder (apart from the amorphous

carbon) being in layers stacked parallel to each other in groups of 2, 3, etc. Above this range of carbon content the fraction of single layers decreases to $\sim 10\%$ at 94% C. The average number of layers in a group increases with increasing rank, particularly rapidly after about 89% C (figure 19). Thus the packing of the layers improves with rank; further, the average separation between layers decreases with increasing rank (figure 21), and the same trend is shown by the r.m.s. variation in spacing (figure 22).

The mean values of interlayer spacing (between about $3 \cdot 6 \text{Å}$ and about $3 \cdot 45 \text{Å}$) are somewhat greater than that for graphite ($3 \cdot 35 \text{Å}$) but still considerably smaller than the average distance of approach of aliphatic chains (4 to 5Å; see, for example, Bragg & Bragg 1933). It follows that those layers which are packed parallel to each other are little disturbed by the possible presence of aliphatic side groups; the latter are therefore either attached to the single layers, or, if attached to the packed layers they must lie outside the stack. This suggests that at least for the packed layers some of the cross-links are in the form of direct C—C linkages, rather than of aliphatic bridges.

The general improvement of the packing and the decrease in interlayer spacing with increasing rank are in good agreement with the conclusions reached above, namely that with increasing rank the buckled sheets become flatter. Furthermore, the suggestion of linkage by direct C—C bonds is consistent with the previous deductions. The buckled imperfect sheets are thought to be arranged as shown schematically in figure 15, the sheets packing parallel to each other over locally flat regions.

7·1·5. *Structural information from the low-angle scattering*

Finally, we consider the scattering at low angles. The nature of this scattering has been discussed previously (Hirsch 1954). The diffuse low-angle scattering extends to very small angles, and the intensity decreases with increasing rank reaching a minimum at 90% C, and after this point it increases again (see figure 1). This variation correlates with porosity (King & Wilkins 1944) and this suggests that the diffuse low-angle scattering is due to pores. The nature of the scattering curves indicates the presence of a wide distribution of pore sizes, while examination of the anisotropy of the scattering from coal sections cut parallel and perpendicular to the bedding plane led to the conclusion that some of the pores are in the form of disk-like cracks parallel to the bedding plane.

For coals with carbon content around 90%, a band occurs at a spacing of about 20Å (figures $1b$, 23; Riley 1944, Nelson 1954, Hirsch 1954; see also table 3). The existence of this band implies that there must be a variation of density on this scale. Fourier analysis of the '20Å' band, and also direct examination of the intensity distribution, leads to the view that the band is due to a central nucleus of about 8Å diameter, whose density is either higher or lower than the average, surrounded by a region of diameter about 20Å, whose density is respectively lower or higher than the average (Brown & Hirsch 1955). These units may occur at random positions in the coals, or they may be close packed as in a liquid, but the Fourier transforms leave little doubt that if any such packing occurs, the units are packed at various distances from each other, the only condition being that they cannot approach closer than their diameter (about 20Å). Examination of the '20Å' band from sections cut parallel and perpendicular to the bedding plane showed that the change in density occurs certainly in the plane of the layers, but that there may also

be a similar change in density normal to the plane of the layers. Since the average layer diameter as determined from analysis of the high-angle diffraction bands is about 7.5Å, it is probable that the diameter of the nucleus is to be identified with that of the layer; it should be noted, however, that some of the layers are known to pack at about 3.5Å parallel to each other; the local density of such a stack is near that of graphite (actually about 2.14 g/cm^3) and therefore considerably greater than the average density. It is therefore very likely that the nucleus is to be identified with a stack of layers, probably consisting of two layers since these occur most frequently (see appendix III). The thickness of a stack of two layers is also ~ 7Å, i.e. approximately equal to the diameter of the nucleus. We believe therefore that the '20Å' band is due to a unit consisting of a nucleus in the form of a stack of approximately two layers, surrounded by other single layers cross-linked to the layers of the nucleus, and also by amorphous material (for diagram see figure 15 and also Brown & Hirsch 1955). This unit can be described simply in terms of the imperfect sheet structure discussed above. The nucleus of diameter 8Å corresponds to the local region of parallel packing of two such layers; the fact that the diameter of the nucleus is nearly equal to $\overline{L}$ is consistent with the assumption made in the discussion of the histograms that the buckled sheet consists of relatively flat regions of diameter $\overline{L}$ linked to others by linkages causing local bends. The nature of the '20Å' band therefore lends support to the idea that $\overline{L}$ really does represent the diameter of a physical entity in the form of a relatively flat layer. The diameter ~ 20Å probably corresponds to the overall size of the buckled sheet, but it is possible of course that the cross-linking extends over larger distances. The absence of diffuse low-angle scattering in this region suggests that cross-links between neighbouring sheets have been removed, so that the sheets have been sufficiently free to move around to pack in a more orderly manner. The flexibility of this structure (previously termed 'liquid structure' (Hirsch 1954)) explains the relatively high fluidity of the coking coals in the softening range (Brown & Hirsch 1955). This appears to correlate with the absence of hydrogen-bonded OH groups.

The strong diffuse scattering in the anthracites supports the conclusion reached above that in this structure the layers are rigidly and extensively cross-linked by direct C—C bonds with the result that macropores are formed. The disappearance of a '20Å' band in the high-rank anthracites (94.1% C) suggests cross-linking between adjacent sheets.

7·2. Lignites

Figure 6 shows that apart from the considerable amount of amorphous material virtually only layers belonging to the smallest size groups are present. The average number of atoms per layer is only 8 to 9, and this suggests that the layers in the lignites contain mainly single substituted benzene rings. These are probably again cross-linked either to form a buckled sheet or a three-dimensional structure. The bond lengths are short (figure 11) and of the order of magnitude expected from single benzene rings. Substitution by aliphatic material would lead to a larger bond length than observed, and this suggests either the presence of many other groups of low bond length (e.g. C=O) or that the layers form buckled sheets as in vitrains. It is interesting to note that some of the histograms, for example, for coals DB and DF, show negative and positive 'ghost' terms typical of a rather narrow distribution, similar to the histogram from benzene (see III).

It should be noted that the number of atoms given above is that corresponding to the equivalent perfect layer, and should therefore be considered as a minimum number of a possibly larger and imperfect layer. No measurements have been made of the discrepancy in the region of the 10 band for the lignites.

The scattering at lower angles shows that these units are packed at distances of about 4 Å (figure 25). The band corresponding to this spacing is somewhat similar to the γ band found for exinite and is very broad, suggesting that it is either due to an average nearest-neighbour distance between the units, which according to figure 10 have diameters of only ~ 5 Å, or due to packing of buckled sheets. Figure 25 shows typical low- and intermediate-angle scattering curves from a number of lignites of different rank. With increasing carbon content there is a tendency for this band to have superimposed on it a rather weak band occurring at $s \sim 0.27 \text{Å}^{-1}$, i.e. close to the position of the 002 band. There is thus a gradual development of the 002 band, while the band at 4 Å disappears around 80 % C. A trace of this band can still be seen for the vitrain HA (78 % C). An interesting feature of these curves is the rather high value of intensity at the high-angle end of the band at 4 Å; in this respect this band differs from the γ band from exinite which is nearly symmetrical (see figure 23 a). This might possibly be due to the presence of a rather high proportion of water in these lignites, which would give rise to a peak near this region (Bernal & Fowler 1935). Low-rank lignites show weak diffuse low-angle scattering, but the intensity increases with rank and approaches that found for the low-rank vitrains; in a few cases a very weak band has been observed in the region of about 12 Å (see figure 25; table 3). It is not clear, however, whether this band is to be interpreted in a manner similar to the '20 Å' band from vitrains, or whether it represents a repeat distance; no detailed analysis has been made.

Since it is sometimes thought that lignin is the starting point of the coalification process (for discussion see Van Krevelen & Schuyer 1957) it was thought worthwhile to examine samples of this material. These were very kindly provided by Dr R. H. Farmer of the D.S.I.R. Forest Products Research Laboratory, Princes Risborough. Figure 6 shows the histogram obtained from a beech lignin, and the other relevant parameters are given on figures 10 to 12. The remarkable fact about this histogram is that the 'layers' contain a larger number of atoms (about 14) than those of the lignites (about 8 or 9). More lignins should be examined before any definite conclusions can be reached. It is believed that further X-ray diffraction studies on lignins and related materials might help to clarify the first stages of the coalification process. It should also be noted that quantitative comparison of the diffraction patterns or of the histograms from lignins with those calculated from theoretical models should help to confirm possible structures of lignin, such as those put forward by Freudenberg (1950), Erdtman (1950) or Fuchs (1931).

At low angles the diffraction patterns of lignins are similar to those of lignites. A weak band occurs at a spacing of ~ 10 Å (see table 3) but no detailed interpretation of this band has been made.

7·3. The coalification process

The results from the lignites, vitrains and anthracites show gradual changes with rank, in agreement with the usually accepted idea that these materials form members of a continuous metamorphic series. According to these results, the coalification process can be divided into several stages. In the first stage, up to about 75 % C, the structure of the

lignites appears to be rather similar, at least as regards the size of the layers. The average number of atoms per layer (assumed perfect) is about 8 to 9, corresponding probably to cross-linked single substituted benzene ring type structures. In this stage, however, the increase in the intensity of diffuse low-angle scattering is taken as an indication of the progressive rigid cross-linking of the units. The second stage extends from about 75% C to about 80% C and is marked by a rapid increase in the average number of atoms per layer to about 15 or 16. This suggests a condensation of the lignite units in this region to form larger aromatic systems. This increase could be accounted for by a condensation of two lignite units to form naphthalene type systems. As has already been pointed out in §7·1 the perfect layers in this range of vitrains contain probably only about two condensed aromatic rings on the average; however, all the evidence discussed in §7·1 suggests that these layers form part of rather larger structures, in the form of imperfect buckled sheets; we believe therefore that in this stage of the coalification process rather extensive condensation or aromatization takes place to form these large structures which, however, are made up of cross-linked perfect subunits containing probably only two condensed aromatic rings on the average. The evidence from the packing of the molecules is consistent with this view; the broad band at 4Å typical of the packing of small molecules (or of heavily buckled sheets) in the lignites below 75%C is replaced at 80% C by the 002 band typical of the parallel packing or rather larger, relatively flat layers. The third stage of the coalification process extends from about 80% C to about 90% C and is characterized by a small increase in the number of atoms per layer (~ 18 at 90% C), improvement in the packing, a decrease in the amorphous material and an increase in the bond length. As has already been mentioned, these changes can be accounted for by a 'flattening' of the sheets by removal of some of the imperfections or groups responsible for the buckles, or changes in orientation, such as —CH_2— bridges and hydrogen-bonded OH groups (deduced from infra-red data; Brown 1955). The decrease in diffuse low-angle scattering in this range suggests that some of the cross-links between buckled sheets are removed so that they can pack better, filling up the macropores and giving rise to the band at ~ 20Å. This 'depolymerization' is probably partly due to the removal of hydrogen-bonded OH groups in this range (Brown 1955; Brown & Hirsch 1955).

The last stage of the coalification process from about 90% C is characterized by a very rapid increase in the size of the layers. This growth of the layers appears to be due partly to a drastic process of perfection inside the cluster units by removal of CH_2 groups and partly to a coalescence of layers in neighbouring clusters, as shown by the progressive disappearance of the band at ~ 20Å. The amorphous material also decreases rapidly with increasing rank in agreement with the removal of much of the aliphatic material in this region (Brown 1955). Extensive cross-linking by direct C—C linkage probably leads to the formation of pores and to the diffuse low-angle scattering associated with this porosity.

7·4. *Comparison of different macerals*

Since the different macerals (vitrinite, exinite, micrinite, fusinite) differ in composition and physical and chemical properties (for review see Van Krevelen & Schuyer 1957), it was thought worth while to examine these with a view to finding any possible differences in the X-ray diffraction patterns. The vitrains described in §7·1 contained a high

proportion of vitrinite; a series of black and grey durains contained various proportions of exinite and micrinite, and included two specimens of almost pure exinite and one specimen of almost pure micrinite (see appendix I). Two specimens of fusain containing mainly fusinite were also examined.

7·4·1. *Black (exinite-rich) durains*

Figure 10 shows that both exinite concentrates have rather smaller layer diameters than vitrains of comparable carbon content. Of the other four exinite-rich durains with carbon content less than about 90 % C, three have smaller layer diameters than the corresponding vitrain; the fourth (HQ) has a rather high proportion of micrinite (nearly 30 %; see appendix I) and this is likely to account for the rather larger value of $\bar{L}$ in this case. The two specimens above 90 % C (HT, HU) actually contain mainly micrinite and vitrinite, and cannot be considered as representative of exinite of this rank.

These results show therefore that exinites with less than about 88 % C have layers which are somewhat smaller than those of the corresponding vitrinites. These results are in qualitative agreement with those deduced by Van Krevelen and his colleagues from their statistical structural analysis (for review see Van Krevelen & Schuyer 1957). Furthermore, figure 12 shows that the low-rank exinite-rich durains contain rather more amorphous material than corresponding vitrains. This result agrees with that obtained from infra-red spectroscopy, where it was found that exinite-rich coals contain more aliphatic material (Brown 1955, see also, Van Krevelen & Schuyer 1957) and this fact also correlates well with the higher hydrogen content of the exinites (see appendix I). Apart from these differences, the histograms and bond lengths are found to be similar to those of the vitrains (see figures 7, 11). It is clear therefore that the layers in exinite-rich coals are similar to but rather smaller than those in vitrains of corresponding rank, and that they probably contain more aliphatic edge groups or aliphatic or alicyclic bridges. The fact that the bond length is similar to that in vitrains suggests that part of the aliphatic material causes the sheets of linked layers to be more buckled than in the vitrains, and part is probably substituted around the free periphery of the layers leading to a compensating increase in bond length. It should be emphasized, however, that exinite-rich coals do not consist of purely hydro-aromatic layers in which the rings are arranged in chair configurations; intensity curves calculated from molecules of this type have a peak in a slightly different position corresponding to a mean effective bond length much larger than that observed. Recent similar calculations by Ergun & Tiensuu (1959) confirm these results. These authors however state that for other configurations of alicyclic ring systems 'the displacement (of the 11 band) is less or even non-existent'. They suggest, therefore, that coals or coal components rich in hydrogen may contain appreciable amounts of alicyclic structures. It should be noted that one of the important features of the diffraction patterns from coals (including exinite) is the fact that the average bond lengths are even lower than that expected from perfect aromatic systems (see §7·1, also figure 11). It remains to be proved whether such low values of bond lengths can be explained in terms of purely alicyclic ring systems. There is, however, little doubt that the low values of bond lengths, and all the other data discussed in this and previous sections, can be explained in terms of the buckled-sheet model developed in the present paper, in which small aromatic layers are linked to

each other by aliphatic or alicyclic bridges or by five-membered rings. The presence of appreciable amounts of such material to produce the buckling is essential in the present model.

As already reported previously (Nelson 1954; Cartz, *et al.* 1956) black durains generally show the broad γ band (first reported by Blayden, Gibson & Riley 1944) at about 4 to 5 Å, as well as a 002 band. It was also shown previously that the γ band appears to be associated with exinite while the 002 band is associated with micrinite (or vitrinite). The γ band of the exinite concentrate *HN* is compared with the 002 band from a corresponding vitrain in figure 23 *a*. The spacing of the γ band is similar to the distance of close packing of aliphatic chains in paraffin crystals (see, for example, Bragg & Bragg 1933), and this suggests that the γ band is due to rather badly packed buckled layers which are prevented from approaching more closely by the presence of the buckles due to alicyclic and peripheral aliphatic material. The occurrence of the γ band is therefore consistent with the deductions made from the analysis of the high-angle diffraction and infra-red spectroscopy data that the layers are probably more buckled and certainly richer in aliphatic material than those of corresponding vitrains.

For the low-rank durains the intensity of the diffuse low-angle scattering appears to be somewhat less than that for the corresponding vitrains, suggesting a lower porosity.

7·4·2. *Grey (micrinite-rich) durains*

The grey durains appear to be even more similar to the vitrains than the black durains. Thus the histograms of *HV*, *HW* and *HX* are all very similar to those of the corresponding vitrains (figures 5, 7). The same is true of $\bar{L}$, the amorphous term and the average bond length. However, in the case of the only micrinite concentrate examined (*HY*), the histogram is rather similar to that of an anthracite; the layer diameter is considerably larger and the amorphous term smaller than for the corresponding vitrain. Furthermore, the discrepancy in the region of the 10 band is considerably smaller than in the case of the anthracite (see table 1). This suggests strongly that the layers are probably considerably more perfect in the micrinite concentrate, so that there is less buckling. This result correlates with the smaller fraction of aliphatic carbon in micrinites (see Van Krevelen & Schuyer 1957) and the smaller hydrogen content. It should be noted that the average number of atoms per layer in the micrinite is 24·8, which, according to the degree of substitution, probably corresponds to 4 to 6 condensed aromatic rings. It appears therefore that this material contains rather more extensively and perfectly condensed aromatic ring systems than the corresponding vitrains. It is not clear, however, why the bond length (1·402 Å) should be so comparatively low.

Although the 002 band from micrinite appears to be rather sharper than that from a corresponding vitrain (see figure 23 *b*), this sharpness appears to be mainly due to a wider distribution in the histogram describing the packing of the layers (figure 18). The most significant feature about this 002 band is that it occurs at a slightly lower spacing than the 002 band from a corresponding vitrain. This is shown in figure 23 *b*. Thus the layers in micrinite appear to pack at a slightly closer distance than in vitrinite, in agreement with the above evidence for greater perfection. Although no detailed analysis of the 002 band has been carried out for the other grey durains, the photographs show clearly that the

002 bands from the grey durains are always sharper than those from corresponding vitrains; this is particularly marked for the low-rank durains. These results suggest that for all the grey durains examined the layers are more perfect than those of corresponding vitrains. Nevertheless, the histograms of the layer size distributions for all the grey durains, except for the micrinite concentrate, are similar to those of corresponding vitrains, and $\bar{L}$ has similar values. It is felt that other micrinite concentrates should be examined before this anomaly can be resolved, although the presence of five-membered rings might account for the results.

At low angles the diffraction patterns from grey durains are similar to those from vitrains and undergo similar changes with variation in rank. Thus, with increasing rank the diffuse low-angle scattering decreases and is replaced by a band at about 20 Å (for photographs see Cartz *et al.* 1956). The grey durains do not show any γ band, although they may contain appreciable amounts of exinite (for example, *HV*); see appendix I. This may be due to the fact that the intensity of the γ band is too weak to be detected (see §5·2). However, no quantitative tests have been carried out to check whether the relative intensities of the 002 and γ bands in any of these durains are compatible with the petrographic analyses.

7·4·3. *Fusains*

Only two fusains were examined (*HZ*, *DA*). One of these (*HZ*) has a larger layer diameter than the corresponding vitrains; the other has not. However, both histograms show a tendency for bimodal distributions not found in the vitrains (see figures 5, 8). In fact the histograms are similar to those found for low-rank coals carbonized at temperatures in the range 600 to 800 °C (see Diamond III; figure 6). Figure 23c shows that the fusain *HZ* tends to have more diffuse low-angle scattering and does not show the band at 20 Å which is so pronounced in the corresponding vitrain, *HH*. The fusain *DA* also shows more diffuse low-angle scattering and less of the '20 Å' band than the corresponding anthracite. The total low-angle scattering measured with a double-crystal spectrometer (see Hirsch 1954) is also found to be much larger for fusain *DA* than for the corresponding vitrain. This indicates that fusains are more porous than anthracites; further, this larger diffuse scattering and the lack of a band at 20 Å are also characteristic of carbonized coals (see III), although it should be noted that the low-angle scattering of the fusains is somewhat less than that of the carbonized vitrains. We conclude that the structure of fusains is generally rather similar to that of a low-rank coal carbonized at temperatures of 600 to 800 °C, and this conclusion is in agreement with the generally accepted fact that fusains are formed at a relatively high temperature, possibly by a process of pyrolysis (see, for examples, Van Krevelen & Schuyer 1957).

7·4·4. *Conclusions*

These experiments have shown that the different macerals, particularly the vitrinites, exinites and micrinites, show distinct differences in their X-ray diffraction patterns, and that they are structurally distinct phases. While the layer structure appears to be substantially similar in all the macerals, the exinites have layers which are smaller and probably more buckled and imperfect (due to aliphatic or alicyclic groups), than those of the vitrinites. They contain more amorphous material. On the other hand, the micrinites

appear to have layers which are probably more perfect and flatter, and which are either equal in size to or larger than those in the vitrinites. The layers in the exinites, which are thought to be very buckled, pack badly (γ band); the more perfect layers in the micrinites pack better than those in the corresponding vitrinites. There appears to be a consistent correlation between the hydrogen content, aliphatic material, the perfection of the layers and the nature of the packing; thus the greater the hydrogen content, the greater is the amount of aliphatic material and the degree of buckling, and the worse is the packing of the layers.

The fusains are again different; thus they have structural parameters which are somewhat similar to those of a low-rank coal carbonized to 600 to 800 °C.

7·5. *Ethylene diamine extracts*

A number of ethylene diamine extracts were prepared from the series of vitrains examined in the present work by the B.C.U.R.A. We are indebted to Dr Dryden, Dr Given and their colleagues for providing these samples. Details of these extracts are given in appendix I. Figure 9 shows the histograms of the extracts compared with those of the original coals. With one exception (coal *HE*) the extracts are effectively indistinguishable from the original coals. In the case of coal *HE*, however, only a very small amount of material could be extracted and this appears to differ from that of the original material. In all other cases, where appreciable amounts could be extracted, the structure of the extract appears to be identical to that of the original coal. This implies either that a fully representative part of the coal is extracted, or that the structural units are all very similar. A similar conclusion was reached by Brown (1955) on the basis of infra-red spectroscopic studies. This does seem to justify the use of ethylene diamine extracts to study coal structure.

The extracts, residues and original coals do show, however, important differences in the scattering at intermediate and low angles (Cartz *et al.* 1956). Thus it was found in the case of the lowest-rank coals examined *HA*, that the low-angle scattering in the extract and residue is considerably smaller, and that a new band appears in the extract at about 12Å (see table 3). The residues show in the case of the low-rank coals a marked increase in the broadening and a movement to lower angles of the 002 band. There appears therefore to be an expansion of the residue normal to the plane of the layers, and further, the lack of low-angle scattering implies that some of the larger pores are closed. For coal *HC* a band appears at about 16Å in the extract, which is not present in the original coal; for coal *HE*, the band at $\sim$ 20Å in the original coal is replaced by one at about 30Å in the extract. However, as already mentioned, this extract consists of only a small fraction of the original coal and may therefore not be representative.

One conclusion to be drawn from these experiments is that the low-angle scattering does not seem to be related to the structure or size of the layers or clusters, but rather to their mode of aggregation. The significance of the rather weak bands occurring at low angles in some of the extracts is not clear; no detailed analysis has been carried out.

7·6. *Pitch*

It was of interest to examine a specimen of pitch for which structural parameters had been determined by Van Krevelen and his colleagues, using the statistical structure analysis (table 4). The X-ray diffraction pattern is similar to that of a vitrain; however, the

average number of atoms per layer (15·7) is found to be smaller than that for a vitrain of comparable carbon content (~ 20) (see appendix II). The presence of the 002 (see figure 23d) shows that some of the layers are packed parallel to each other; the average degree of packing is somewhat similar to that of a corresponding vitrain, although the shape of the 002 band and therefore also that of the histogram are different. Table 1 shows that the discrepancy in the 10 region is rather large for the pitch (DO) and this suggests the presence of considerable strain in the layers. An important difference between the low-angle diffraction patterns from the pitch and the corresponding vitrain is that for the former a weak band occurs at an angle corresponding to a spacing of ~ 10Å, instead of ~ 20Å for the vitrain. By analogy with the interpretation of the band at ~ 20Å, it is suggested that the overall diameter of the imperfect unit in the pitch is about 10Å. Since in this case this diameter is not much greater than $\bar{L}$ (7Å), the discrepancy in the 10 region probably corresponds to that from a strained layer of 10Å diameter; according to the estimate of the effect of strain on $\bar{L}$ reported in §4·3, it is reasonable to suppose that a discrepancy of 1·2 electron units could account for the difference ($=3$Å) between 10Å and $\bar{L}$. (Further evidence to support this estimate will be reported in §7·7.) We believe therefore that pitch DO consists of imperfect sheets of ~ 10Å diameter corresponding to ~ 32 atoms. This may be compared with Van Krevelen's estimate of ~ 30 atoms in the cluster and ~ 27 aromatic carbon atoms. This example shows how important the effect of strain can be in causing the true number of atoms in the whole imperfect unit to be underestimated.

7·7. *Co-precipitate of three quinones*

The preparation of this material has already been described in §4·5; the molecules are shown in figure 14. This co-precipitate was examined for two reasons: (1) It has been suggested that the dark colour of coal is due to some charge transfer effect between parallel packed layers (Schuyer 1956). It is found in practice that the co-precipitate of quinones has a much darker colour than the single mixture (Akamatsu & Nagamatsu 1947). It was thought necessary therefore to examine the co-precipitate from a structural point of view to study particularly the nature of the packing. (2) Since the molecular structures were known, the co-precipitate should act as a good model substance to test the methods of analysis.

The diffraction pattern consists of two-dimensional diffraction bands at high angles, a 002 band at intermediate angles and three weak bands at low angles (see table 3; also figure 24). Figure 14 shows the histogram obtained from the high-angle bands, compared with the histogram expected from pyranthrone, which represents a good average of the three molecules. It is clear that the two histograms are considerably different. While part of this difference could be due to the presence of impurities, particularly in the form of smaller molecules, the discrepancy in the average number of atoms is too large to be accounted for completely in this way. Part of the amorphous term may be due to water still present in the material. The clue to the origin of this inconsistency comes from the discrepancy in the region of the 10 band, which in this case is found to be quite large (1 electron unit according to table 1). We suggest therefore that in the co-precipitate the layers are somewhat strained and bent; comparing the above discrepancy with that found for the strained molecule discussed in §4·3, it may be concluded that for a discrepancy of

~ 1 electron unit, a reduction of $\bar{L}$ by $\sim 2\text{Å}$ is quite reasonable. This lends support to the interpretation of the pitch DO discussed in §7·6.

The bands at low angles (figure 24, table 3) are due to the packing of the molecules side by side. Thus the broad band at an angle corresponding to a spacing of about 8Å corresponds to the smallest spacing between the layers when packed with their long dimension parallel to each other, the width of the molecules being about 8Å. The similarity between the diffraction patterns, and in particular the histograms and positions of the low-angle bands for the pitch DO and those for the co-precipitate of three quinones suggests that the size and arrangement of the units in the two substances are rather similar, although the molecules may be chemically different.

8. Conclusions

The main object of the X-ray studies was to attempt to determine a detailed structural model of coal. The presence of imperfections in the layers, however, makes it impossible to deduce an unambiguous structure. Nevertheless, considering all the evidence together we conclude that the structural units in bituminous coals consist of small condensed aromatic ring systems of probably 1 to 3 rings for low-rank vitrains and 2 to 5 rings for vitrains with 90% C, these aromatic layers being linked to each other by direct C—C linkages and aliphatic groups (or possibly also by ether linkages) to form larger imperfect sheets which are either buckled (through the presence of hydroaromatic groups), or in which adjacent aromatic ring systems are rotated relative to each other about an axis normal to the plane of the sheets (for example, as a result of the presence of five-membered rings). The diameters of the aromatic layers are about 7 to 8Å; the imperfect sheets are probably considerably larger; thus, for vitrains with $\sim 90\%$ C these sheets probably extend over $\sim 20\text{Å}$, or possibly even over larger distances. The sheets are also considered to have side groups in the form of short aliphatic chains, OH, and quinone groups, evidence for which is available from other data (see Dryden 1958). Figure 27 shows an example of a type of molecule which is thought to be consistent with most of the experimental facts relevant to a vitrain of $\sim 84·5\%$ C. Table 5 shows the structural data of this molecule. The composition is similar to that of a vitrain; the ratio $C_{ar.}/C$, where $C_{ar.}$ and C are respectively the aromatic and total number of carbon atoms per molecule, is only a little larger than the value estimated from infra-red spectroscopic data (Brown & Hirsch 1955; see also figure 26); the values of $H_{ar.}/C$ and $H_{al.}/C$, where $H_{ar.}$ and $H_{al.}$ are respectively the number of aromatic and aliphatic hydrogen atoms per molecule, are also consistent with these data. The ratios $C_{ar.}/C$ and R/C, where R is the total number of rings per molecule, are also in good agreement with those deduced by Van Krevelen & Chermin (1954a) from density measurements using the statistical structural analysis. The agreement is not so good with their more recent results deduced by the graphical densimetric method (Van Krevelen & Chermin 1954b). With regard to the size of the molecule, the longest overall diameter is about 20Å, while the average number of atoms diffracting coherently is estimated very approximately to be about 16 (corresponding to the average X-ray layer diameter $\bar{L} = 7\text{Å}$), a value similar to that observed for vitrains of corresponding rank (see appendix 2). The molecular weight is also of a reasonable order of magnitude (Dryden 1958). It should be emphasized, however, that this molecule is presented only for the
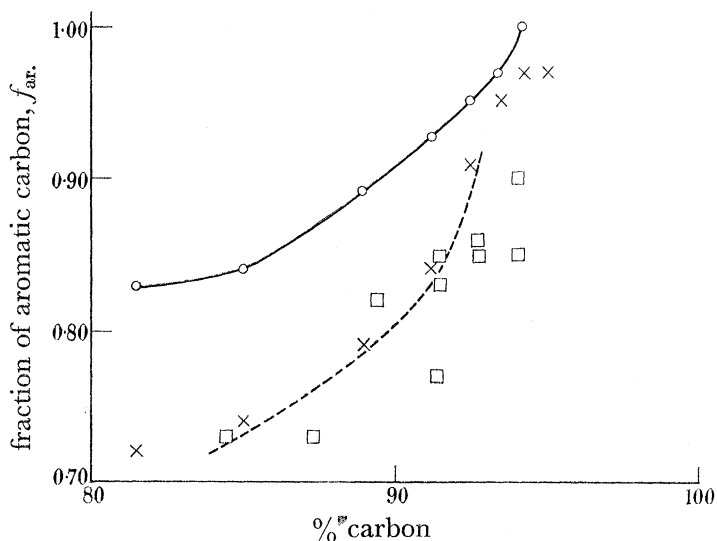
FIGURE 26. Estimates of fraction of aromatic carbon: (a) From infra-red spectroscopy (Brown & Hirsch 1955); dashed curve; (b) from the volatile matter content (Van Krevelen 1953), crosses; (c) from a graphical densitometric analysis (Van Krevelen & Chermin 1954b), solid curve with circular symbols; (d) from present X-ray measurements, being $1 - A$, square symbols.
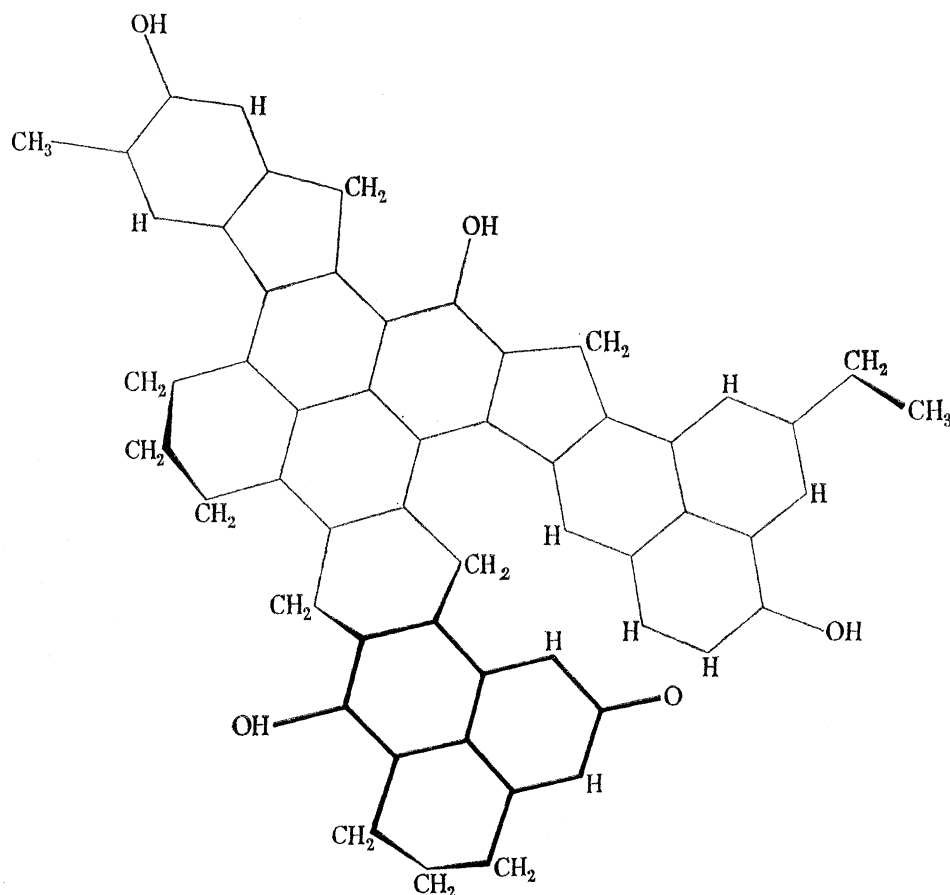

FIGURE 27. A type of molecule consistent with the experimental data for a vitrain of about 84·5 % carbon; see §8 and table 5. The heavier lines represent atomic linkages out of the plane of the diagram.

purpose of indicating the type of structure which we believe to be compatible with the X-ray and other data. The detailed configurations and the extent of the molecule may be different. A rather similar model has been proposed recently by Given (1959), on consideration of the structural implications of the distribution of hydrogen.

The various macerals appear to have basically similar structures but they differ in the degree of perfection, the size, and in the nature of the packing of the layers. Thus in terms of the molecule in figure 27, exinite would have rather more hydroaromatic rings than the corresponding vitrinite, instead of some benzene or five-membered rings. These differences correlate with the differences in the proportion of aliphatic groups as determined by other techniques.

With regard to the coalification process the X-ray data indicate the existence of several distinct stages which are discussed in detail in §7·3. Above about 90 % C the perfect

TABLE 5. DATA RELEVANT TO THE MOLECULE SHOWN IN FIGURE 27

structural formula		$C_{55}H_{41}O_5$	
molecular weight		781	
composition	C	84·5 %	
	H	5·25 %	
	O	10·25 %	
structural parameters			
total carbon	C	55	
aromatic carbon	$C_{ar.}$	42	$C_{ar.}/C$ 76·4 %
aliphatic carbon	$C_{al.}$	13	$C_{al.}/C$ 23·6 %
aromatic hydrogen	$H_{ar.}$	9	$H_{ar.}/C$ 16·4 %
aliphatic hydrogen	$H_{al.}$	28	$H_{al.}/C$ 50·9 %
phenolic OH		4	
quinone O		1	
total number of rings	R	14	R/C 0·255
number of benzene rings		9	
number of benzene rings linked by direct C—C linkages		7	

Average number of coherently diffracting atoms probably ~ 16.

condensed aromatic layers increase rapidly in size with increasing rank; examination of figure 27 shows that this aromatization process can take place fairly easily at hydroaromatic bridges by removal of hydrogen accompanied by relatively small adjustments in the positions and orientations of adjacent layers; but is likely to be more difficult at five-membered rings. In fact such five-membered rings may still be present in anthracites and even in carbonized coals. It should be noted also that the condensation process probably also involves cross-linking of neighbouring cluster units (see §7·3).

The question arises as to whether the structural model deduced from the X-ray data is also consistent with the results of chemical investigations and with certain other conclusions from statistical structural analyses, not yet discussed. Oxidation and hydrogenation studies have been used to estimate the number of condensed rings in coal molecules. The most recent oxidation studies (Montgomery & Holly 1957; see also review by Horton 1958) seem to suggest that the aromatic layers contain only 1 to 3 condensed benzene rings, but the possibility that larger condensed ring systems are present in the original coal could not be ruled out (Van Krevelen & Schuyer 1957). On the other hand, the results of careful hydrogenation studies of a coal with 86·5 % C (Schuhmacher, Van Vucht, Groenewege,

Blom & Van Krevelen 1956) have been interpreted in terms of condensed aromatic ring systems containing 3 to 11 rings. It has been suggested, however, that complex condensation reactions might take place during hydrogenation (Horton 1958). Other chemical studies are reviewed by Van Krevelen & Schuyer (1957) and by Horton (1958). There still appears therefore to be considerable controversy as to the validity of deductions made about the number of condensed aromatic rings from such studies. It may be noted, however, that the X-ray data are consistent with the oxidation results of Montgomery & Holly (1957).
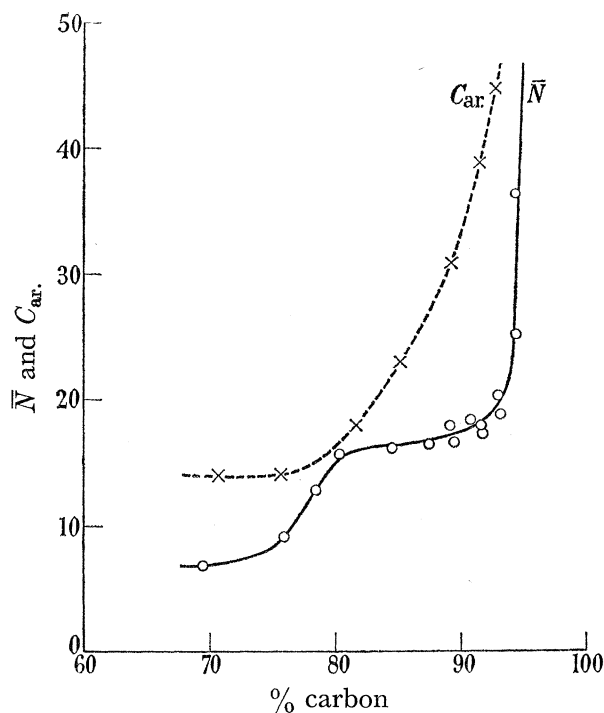

FIGURE 28   FIGURE 29

FIGURE 28. Comparison of the average number of aromatic carbon atoms, $C_{ar.}$ per cluster unit in vitrains (dashed curve) estimated from molar refraction experiments (Van Krevelen & Schuyer 1957) with $\bar{N}$ from the X-ray measurements (solid curve).
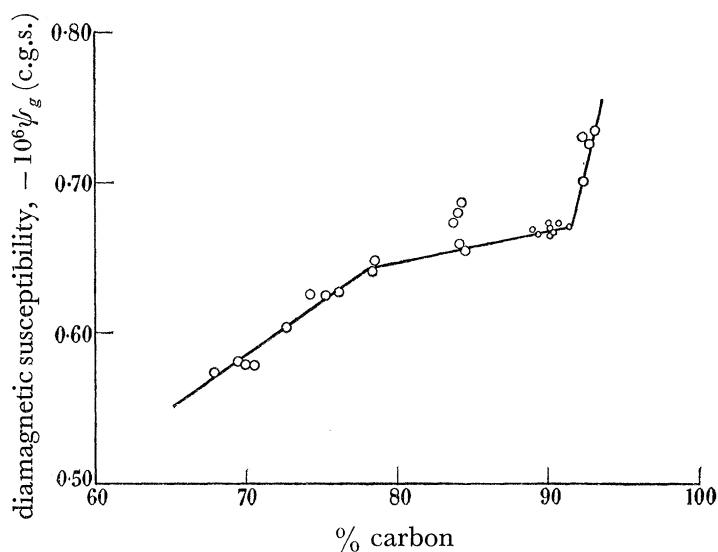
FIGURE 29. The variation of the diamagnetic susceptibility with carbon content for a series of vitrains (Honda & Ouchi 1957).

Schuyer & Van Krevelen (1954) have used values of the molar refraction to determine the aromatic surface and hence an average number of aromatic carbon atoms, $C_{ar.}$, per cluster unit in the coals. These values of $C_{ar.}$ for the vitrains are compared with the number of atoms in a coherently diffracting layer deduced from X-ray data, $\bar{N}$, in figure 28. It is clear that the values of $C_{ar.}$ are larger than those of $\bar{N}$, e.g. by about 20 atoms at 90 % C. This discrepancy is considerable, particularly as $C_{ar.}$ corresponds to the number of atoms in the aromatic surface only, while $\bar{N}$ includes also non-aromatic edge atoms. It is possible that part of the discrepancy is due to strain in the layers, so that they are really larger but imperfect; however, the evidence from the band at 20 Å suggests that the layers are not larger than about 8 Å, corresponding to $\bar{N}$. The differences can be reconciled as follows. It will be seen from the analysis of Schuyer, Blom, & Van Krevelen (1953) and

from the tests carried out on model substances (e.g. fig. VII, 9 of Van Krevelen & Schuyer 1957), that molecules such as pyrene and 1, 2 benzfluorene have the same aromatic surface and similar values of $I_m/C_{ar.}$ where I_m is the molar refractometric increment. It should be emphasized, however, that the presence of the five-membered ring causes a change in orientation of the single benzene ring relative to the naphthalene system (compare figure 27). The calculations described in III on the X-ray scattering from condensed aromatic systems containing five-membered rings indicate that such a molecule will probably appear as a two-ring system, the five-membered ring breaking the coherence of the scattering from the two parts of the molecule. We suggest therefore that the values of $C_{ar.}$ and $\bar{N}$ can be reconciled if the aromatic surface is made up, as in the above case, by small condensed systems consisting perhaps of ~ 1 to 3 rings at 80 % C and ~ 2 to 5 rings at 90 % C, which are linked to each other partly by direct C—C bonds and partly by aliphatic bridges thus causing buckles or changes in orientation of the hexagons in the plane of the layers if five-membered rings are formed. Imperfections of this type occurring in the larger sheets are precisely those inferred from the X-ray data, and are illustrated in figure 27. We conclude therefore that the results of the statistical structural analysis and those of the X-ray studies are compatible with each other, but that the values of $C_{ar.}$ and $\bar{N}$ are not directly comparable. Thus we believe that $\bar{N}$ is the average number of atoms of the coherently scattering unit, while $C_{ar.}$ is the number of aromatic carbon atoms of the aromatic surface effective in determining the contribution to the refractive index due to conjugated double bonds. Neither of these parameters corresponds necessarily to an actual diameter of a molecule or cluster unit. The actual size of the cluster unit must be equal to or larger than, and the size of the perfect condensed aromatic ring system must be smaller than, that corresponding to $\bar{N}$ or $C_{ar.}$.

Measurements of diamagnetic susceptibility by Honda & Ouchi (1957) have been used to estimate directly the number of aromatic rings per cluster unit. By applying an empirical relation due to Schuyer (1955) between total molar diamagnetic susceptibility and the contributions due to different atoms, Van Krevelen & Schuyer (1957) deduce the number of condensed aromatic rings per cluster unit for vitrains of varying carbon content. Figure 29 shows the variation of susceptibility with carbon content according to the measurements of Honda & Ouchi; this curve is somewhat similar to that of $\bar{L}$ against carbon content (see figure 10). The number of aromatic rings deduced by Van Krevelen & Schuyer from these measurements increases from ~ 3 at 75 % C to ~ 9 at 90 % C. It is not clear, however, whether these rings have to be joined to each other to make perfect aromatic lamellae or whether some of them could be joined partly by single C—C linkages and partly by isolated aliphatic groups to form imperfect sheets as in figure 27. In the latter case these results could also be reconciled with the X-ray data.

It appears then from the discussion in this section that the X-ray data can be reconciled with the results of at least some of the other investigations, but each of the different methods used is subject to considerable errors and uncertainties so that the final detailed structural model is still in doubt.

The relation between coal structure and physical and chemical properties of coal has been discussed recently by Van Krevelen & Schuyer (1957), and also in a number of papers contributed to the Sheffield Conference on 'Science in the Use of Coal' (1958). It

should be noted that the reason for the dark colour of coal is still somewhat in doubt (Dryden 1958) although charge transfer effects between parallel layers (Schuyer 1956) and the occurrence of free radicals (Friedel 1957; for recent review on free radicals see Austen & Ingram 1958) might be contributing factors.

With regard to the X-ray technique, it is felt that future research might be carried out profitably along the following lines.

(1) A theoretical investigation of the effect of edge groups on bond lengths, and also further calculations of the intensity curves from particular molecules. Such calculations are being carried out at present (Ruland 1959; Ergun & Tiensuu 1959).

(2) Examination of model substances of known structure; a very successful study of this type has been carried out recently by Ruland (1959). The method could also be applied to pitch, the structure of which seems to be understood better than that of coal.

(3) Correlation between changes in the X-ray patterns and chemical treatment. Such studies are already yielding valuable information (Ruland & Tschamler 1958; for other references see Ergun & Tiensuu 1959).

(4) Further experiments on other macerals and lignites.

We feel however that the X-ray technique can only give limited information by itself and that the problem of the structure of coal can probably only be finally solved by synthesizing molecules which have all the properties of coal.

REFERENCES

Akamatsu, H. & Nagamatsu, K. 1947 *J. Colloid Sci.* **2**, 593.
Austen, D. E. G. & Ingram, D. J. E. 1958 *Proceedings of Conference on Science in the Use of Coal*, p. A 62. London: The Institute of Fuel.
Bernal, J. D. & Fowler, R. H. 1935 *J. Chem. Phys.* **1**, 515.
Blayden, H. E., Gibson, J. & Riley, H. L. 1944 *Proceedings of Conference on the Ultra-fine Structure of Coals and Cokes*, p. 118. London: British Coal Utilization Research Association.
Bradley, A. J. 1935 *Proc. Phys. Soc.* **47**, 879.
Bragg, W. H. & Bragg, W. L. 1933 *The crystalline state*, vol. I, p. 167. London: Bell.
Brown, J. K. 1955 *J. Chem. Soc.* 744.
Brown, J. K. & Hirsch, P. B. 1955 *Nature, Lond.* **175**, 229.
Cartz, L., Diamond, R. & Hirsch, P. B. 1956 *Nature, Lond.* **177**, 500.
Compton, A. H. & Allison, S. K. 1935 *X-rays in theory and experiment*, p. 782. New York: Van Nostrand.
Diamond, R. 1956 Ph.D. dissertation, University of Cambridge.
Diamond, R. 1957 *Acta Cryst.* **10**, 359.
Diamond, R. 1958 *Acta Cryst.* **11**, 129.
Diamond, R. 1959 *Phil. Trans.* A, **252**, 193.
Dryden, I. G. C. 1951 a *Fuel*, **30**, 39.
Dryden, I. G. C. 1951 b *Fuel*, **30**, 145.
Dryden, I. G. C. 1951 c *Fuel*, **30**, 217.
Dryden, I. G. C. 1952 *Fuel*, **31**, 176.
Dryden, I. G. C. 1958 *Proceedings of Conference on Science in the Use of Coal*, p. A 13. London: The Institute of Fuel.
Erdtman, H. 1950 *Research, Lond.* **3**, 63.
Ergun, S. & Tiensuu, V. H. 1959 *Nature, Lond.* **183**, 1668.
Franklin, R. E. 1950 *Acta Cryst.* **3**, 107.

Franklin, R. E. 1951 *Proc. Roy. Soc.* A, **209**, 196.

Freudenberg, K. 1950 *Angew. Chem.* **62**, 30.

Friedel, R. A. 1957 *Nature, Lond.* **179**, 1237.

Fuchs, W. 1931 *Die Chemie der Kohle.* Berlin.

Given, P. H. 1959 *Nature, Lond.* **184**, 980.

Hirsch, P. B. 1954 *Proc. Roy. Soc.* A, **226**, 143.

Hirsch, P. B. 1958 *Proceedings of Conference on Science in the Use of Coal*, p. A29. London: The Institute of Fuel.

Honda, H. & Ouchi, K. 1957 *Fuel*, **36**, 159.

Horton, L. 1958 *Proceedings of Conference on Science in the Use of Coal*, p. A24. London: The Institute of Fuel.

Keating, D. T. & Vineyard, G. H. 1956 *Acta Cryst.* **9**, 895.

King, J. G. & Wilkins, E. T. 1944 *Proceedings of Conference on the Ultra-fine Structure of Coals and Cokes*, p. 46. London: British Coal Utilization Research Association.

Montgomery, R. S. & Holly, E. D. 1957 *Fuel*, **36**, 63.

Nelson, J. B. 1954 *Fuel*, **33**, 153.

Peiser, H. S., Rooksby, H. P. & Wilson, A. J. C. 1954 *X-ray diffraction of polycrystalline materials*, p. 130. London: Institute of Physics.

Riley, D. P. 1944 *Proceedings of Conference on the Ultra-fine Structure of Coals and Cokes*, p. 232. London: British Coal Utilization Research Association.

Robertson, J. M. 1953 *Organic crystals and molecules*, p. 211. Cornell University Press.

Ruland, W. 1959 *Acta Cryst.*, **12**, 679.

Ruland, W. & Tschamler, H. 1958 *BrennstChemie.*, **39**, 363.

Schuhmacher, J. P., Van Vucht, H. A., Groenewege, M. P., Blom, L. & Van Krevelen, D. W. 1956 *Fuel*, **35**, 281.

Schuyer, J. 1955 *Naturwissenschaften*, **42**, 388.

Schuyer, J. 1956 *BrennstChemie*, **37**, 74.

Schuyer, J., Blom, L. & Van Krevelen, D. W. 1953 *Trans. Faraday Soc.* **49**, 1391.

Schuyer, J. & Van Krevelen, D. W. 1954 *Fuel*, **33**, 176.

Van Krevelen, D. W. 1953 *BrennstChemie*, **34**, 167.

Van Krevelen, D. W. & Chermin, H. A. G. 1954*a* *Fuel*, **33**, 79.

Van Krevelen, D. W. & Chermin, H. A. G. 1954*b* *Fuel*, **33**, 338.

Van Krevelen, D. W. & Schuyer, J. 1957 *Coal science*. Amsterdam: Elsevier.

APPENDIX 1. ORIGIN AND ELEMENTARY ANALYSES OF COALS

coal	origin	% C	% H	% volatile matter (d.a.f.)	source	description of coal used by Hirsch (1954)
		(d.m.f.)				
		VITRAINS				
HA	Measham, Eureka Seam	78·3	5·2	42·2	C.S.L.	H
HB	Cannock Wood, Shallow Seam	80·1	5·3	43·1	C.S.L.	G
HC	Monk Bretton, Meltonfield Seam	84·4	5·3	38·5	C.S.L.	F
HD	Grimethorpe, Parkgate Seam	87·3	5·4	34·7	C.S.L.	E
HE	Roddymoor, Five Quarter Seam	89·0	5·0	27·2	C.S.L.	D
HF	Langley Park, Victoria Seam	89·3	5·1	26·4	C.S.L.	C
HG	Coedley, Pentre Seam	90·6	4·9	23·2	C.S.L.	—
HH	Coegnant, Gellideg Seam	91·4	4·4	15·9	C.S.L.	B
HI	Bryn, Gellideg Seam	91·5	4·4	15·2	C.S.L.	—
HJ	Fforchaman, Gellideg Seam	92·8	3·9	9·8	C.S.L.	—
HK	Cwmgwrach, Yard Seam	92·9	3·8	8·3	C.S.L.	—
HL	Llandebie, Middle Seam	94·1	3·1	5·3	C.S.L.	—
HM	Pontyberem, Lower Pumpquart Seam	94·1	3·0	5·3	C.S.L.	A

coal	origin	% C	% H	% volatile matter (d.a.f.)	exinite (%)	carbinite (%)	vitrinite (%)	source	notes
		(d.m.f.)			petrographic constituents				
		DURAINS							
black durains									
HP	Cannock Wood, Shallow Seam	81·5	6·5	62·4	82·5	14·9	2·6	C.S.L.	acid washed
HQ	Rawdon Stockings, Seam	82·4	5·8	52·5	67·5	29·4	3·1	C.S.L.	—
HN	Peckfield, Beeston Seam	83·3	7·1	70·0	91	8	1	C.S.L.	exinite concentrate
HR	Peckfield, Beeston Seam	83·7	6·6	60·1	85·3	13·3	1·4	C.S.L.	—
HO	—	84·5	6·6	—	95	5	—	D.S.M.	exinite concentrate (supplied by Professor Van Krevelen)
HS	Aldwarke Silk-stone Branch Seam	87·9	6·3	50·5	71·0	26·0	3·0	C.S.L.	—
HT	North Gelynen, Old Coal Seam	90·8	4·7	20·3	44	42	14	C.S.L.	—
HU	Waunllwyd, Meadow Vein Seam	90·9	4·6	18·9	36	42	20	C.S.L.	—
grey durains									
HV	Baddesley Two Yard Seam	82·3	4·9	38·2	32·2	58·8	9·0	C.S.L.	—
HY	Kiveton Park, Barnsley Seam	86·5	4·0	23·5	9	83	8	C.S.L.	micrinite concentrate; acid washed
HW	Sixbells, Big Seam	90·4	4·5	18·9	20	68	12	C.S.L.	—
HX	Oakdale Yard Seam	91·4	4·4	16·4	12	57	22	C.S.L.	—
		FUSAINS							
HZ	Manvers, Winter Seam	91·4	2·8	12·9	—	—	—	C.S.L.	acid washed
DA	Bearpark, Victoria Seam	93·1	3·6	13·9	—	—	—	C.S.L.	acid washed

coal	origin	% C	% H	% volatile matter (d.a.f.)	source	notes
		(d.m.f.)				
		LIGNITES				
DB	Irish Dopplerite	58·5	4·7	—	C.S.L.	—
DD	Weich-braunkohle Grube Wachtberg (Köln)	65·0	4·7	56·0	C.S.L.	Supplied by Drs Stach & Teichmüller
DE	Liblar/Köln Grube Liblar, Flöz IV	69·5	4·9	54·6	C.S.L.	(X)
DF	Beran, Borneo	75·9	5·3	—	D.S.M.	(H)
		VITRAIN EXTRACTS				
DG	Measham Colliery, Eureka Seam	—	—	—	B.C.U.R.A.	ethylene diamine extract from HA
DH	Cannock Wood, Shallow Seam	—	—	—	B.C.U.R.A.	ethylene diamine extract from HB
DI	Monk Bretton, Meltonfield Seam	—	—	—	B.C.U.R.A.	ethylene diamine extract from HC
DJ	Grimethorpe, Parkgate Seam	—	—	—	B.C.U.R.A.	ethylene diamine extract from HD
DK	Roddymoor, Five Quarter Seam	—	—	—	B.C.U.R.A.	ethylene diamine extract from HE
		MISCELLANEOUS				
DC	Beech Lignin	60·1	5·4	—	—	(I)
DM	Yugoslavia (Istria) Rasa high sulphur coal	77·3	5·6	50·1	C.S.L.	acid washed; contains 12% sulphur by weight
DO	pitch	92·7	4·4	—	D.S.M.	(H)
DZ	pure carbon	95	—	—	B.C.U.R.A.	Supplied by Dr J. K. Brown

B.C.U.R.A. = British Coal Utilization Research Association, Leatherhead, Surrey.
C.S.L. = Coal Survey Laboratory, National Coal Board, Sheffield.
D.S.M. = Dutch State Mines Central Laboratory, Geleen, Holland.
d.m.f. = dry mineral-free basis.
d.a.f. = dry ash-free basis.
(X) = supplied by Dr Mackowsky.
(H) = supplied by Professor Van Krevelen.
(I) = supplied by Dr Farmer.

APPENDIX 2. NUMERICAL DATA OF THE LAYER-SIZE HISTOGRAMS

(% by weight of C in different size groups)

coal	amorphous material	layer diameter, L(Å) 5·8	8·4	10	15	20	30	$\bar{L}$ (Å)	average bond length, l(Å)	average no. of atoms per layer, $\bar{N}$
VITRAINS										
HA	31	53	18	2	$\bar{5}$	0	1	6·3	1·389	12·8
HB	35	44	19	6	$\bar{4}$	$\bar{2}$	2	7·0	1·393	15·7
HC	27	48	19	6	$\bar{2}$	0	2	7·1	1·400	16·1
HD	27	52	18	2	$\bar{2}$	1	2	7·2	1·393	16·6
HE	23	39	23	14	1	$\bar{1}$	1	7·5	1·397	18·0
HF	18	48	22	10	0	2	0	7·2	1·397	16·6
HG	23	40	22	12	2	1	0	7·6	1·403	18·5
HH	15	47	23	12	2	2	$\bar{1}$	7.5	1·403	18·0
HI	17	50	22	9	0	1	1	7·4	1·403	17·5
HJ	15	36	27	19	4	$\bar{2}$	1	8·0	1·406	20·5
HK	14	44	23	12	5	4	$\bar{2}$	7·7	1·406	19·0
HL	15	36	22	14	7	5	1	8·9	1·406	25·4
HM	10	25	26	22	7	2	8	10·7	1·407	36·6
DURAINS										
black durains										
HP	39	47	14	0	$\bar{2}$	2	0	6·6	1·396	13·9
HQ	39	41	14	2	2	3	$\bar{1}$	7·1	1·401	16·1
HN	35	58	12	$\bar{6}$	$\bar{3}$	6	$\bar{2}$	6·0	1·400	11·5
HR	36	51	13	$\bar{2}$	$\bar{2}$	6	$\bar{2}$	6·5	1·402	13·5
HO	30	64	2	3	1	5	$\bar{5}$	5·5	1·395	9·7
HS	28	61	12	$\bar{6}$	$\bar{2}$	10	$\bar{3}$	6·6	1·399	13·9
HT	17	54	17	3	3	8	$\bar{2}$	7·6	1·406	18·5
HU	18	49	17	5	7	9	$\bar{5}$	7·4	1·406	17·5
grey durains										
HV	28	56	15	$\bar{2}$	$\bar{1}$	4	0	6·9	1·392	15·2
HY	18	24	28	24	6	$\bar{2}$	2	8·8	1·402	24·8
HW	18	62	14	$\bar{3}$	1	10	$\bar{2}$	7·4	1·404	17·5
HX	19	53	19	5	0	3	1	7·5	1·404	18·0
FUSAINS										
HZ	20	37	14	6	9	13	1	10·2	1·405	33·4
DA	15	55	17	2	3	8	0	8·1	1·405	21·0
LIGNITES										
DB	42	74	3	$\overline{21}$	$\bar{6}$	11	$\bar{3}$	5·0	(1·39)	8·0
DD	31	77	$\bar{6}$	$\bar{1}$	$\bar{8}$	14	$\bar{7}$	4·9	(1·385)	7·9
DE	36	71	$\bar{6}$	$\bar{2}$	$\bar{7}$	10	$\bar{6}$	4·6	—	6·8
DF	26	94	2	$\overline{29}$	$\bar{6}$	18	$\bar{5}$	5·3	1·384	9·0
MISCELLANEOUS										
DC	42	49	12	$\bar{2}$	$\bar{3}$	1	1	6·4	1·401	13·2
DM	23	90	5	$\overline{24}$	$\bar{6}$	16	$\bar{4}$	5·6	1·403	10·1
DO	15	59	17	5	4	0	—	7·0	—	15·7
DZ	4	$\overline{16}$	16	28	26	19	23	18·5	1·411	110

602   L. CARTZ AND P. B. HIRSCH ON THE

APPENDIX 3. NUMERICAL DATA OF THE HISTOGRAMS DESCRIBING THE PACKING OF THE LAYERS IN COALS

	amorphous material	% by weight of carbon in stacks containing different numbers of layers — number of layers per stack									$\bar{n}$	average spacing, $\bar{d}$ (Å)	average r.m.s. variation of spacing $\bar{\mu}$ (Å)
		1	2	3	4	5	6	7	8	9			
VITRAINS													
HA	31	41	19	4	5	—	—	—	—	—	1·30	3·52	0·71
HB	35	38	17	6	$\bar{1}$	5	—	—	—	—	1·32	3·50	0·72
HC	27	41	11	10	7	4	—	—	—	—	1·39	3·52	0·78
HD	27	38	15	4	7	3	0	4	2	—	1·46	3·49	0·70
HE	23	21	21	14	4	10	1	1	1	4	1·92	3·49	0·70
HF	18	19	45	$\bar{7}$	12	1	7	5	—	—	1·85	3·46	0·62
HH	15	32	10	19	7	$\bar{1}$	6	8	4	—	1·79	3·50	0·67
HM	10	10	26	15	12	0	25	1	0	1	2·54	3·45	0·62
MICRINITE													
HY	18	48	2	13	10	1	$\bar{2}$	$\bar{9}$	19	—	1·45	3·41	0·50
FUSAINS													
HZ	20	19	20	27	9	5	—	—	—	—	1·94	3·43	0·63
DA	15	40	17	11	7	2	2	5	1	—	1·53	3·52	0·74
PITCH													
DO	15	47	$\bar{27}$	52	3	8	$\bar{4}$	6	—	—	1·59	3·53	—